T.C.

ALTINBAŞ ÜNİVERSİTESİ

Fen Bilimleri Enstitüsü

Elektrik ve Bilgisayar Mühendisliği

EXPERIENCE BASED DYNAMIC INTER-CELLULAR BANDWIDTH SHARING FOR LTE OFDMA NETWORKS

Mert Yağcıoğlu

PhD Thesis

Prof. Dr. Oğuz Bayat

İstanbul, 2019

EXPERIENCE BASED DYNAMIC INTER-CELLULAR BANDWIDTH SHARING FOR LTE OFDMA NETWORKS

by

Mert Yağcıoğlu

Electrical and Computer Engineering

Submitted to the Graduate School of Science and Engineering
in partial fulfillment of the requirements for the degree of
Doctor of Philosophy

ALTINBAŞ UNIVERSITY

2019

This is to certify that we have read this thesis and that in our opinion it is fully adequate, in scope and quality, as a thesis for the degree of Doctor of Philosophy.

_____
Prof. Oğuz BAYAT
Supervisor

Examining Committee Members (first name belongs to the chairperson of the jury and the second name belongs to supervisor)

Asst. Prof. Oğuz ATA	School of Engineering and Natural Sciences, Altınbaş University	_____
Prof. Oğuz BAYAT	School of Engineering and Natural Sciences, Altınbaş University	_____
Asst. Prof. Çağatay AYDIN	School of Engineering and Natural Sciences, Altınbaş University	_____
Prof. Hasan Hüseyin BALIK	Air Force Academy, National Defense University	_____
Asst. Prof. Adil Deniz DURU	Spor Academy, Marmara University	_____

I certify that this thesis satisfies all the requirements as a thesis for the degree of Doctor of Philosophy.

_____
Asst. Prof. Çağatay AYDIN
Head of Department

Approval Date of Graduate School of Science and Engineering: ____/____/____

_____
Prof. Oğuz BAYAT
Director

I hereby declare that all information in this document has been obtained and presented in accordance with academic rules and ethical conduct. I also declare that, as required by these rules and conduct, I have fully cited and referenced all material and results that are not original to this work.

Mert Yağcıoğlu

ACKNOWLEDGEMENT

I am highly thankful to my supervisor Prof. Oğuz Bayat who helped and encouraged me during my thesis, without his support it was hard to complete my thesis. I am dedicating this thesis to my wife and family who supported me during my entire studies at PhD, without their support and motivations I might not be able to come up with my studies. I am also thankful to my friends who gave me company for my entire years of study and their nice attitude and motivations gave a nice environment.

ÖZET

LTE OFDMA AĞLARI İÇİN DENEYİM TABANLI DİNAMİK HÜCRELER ARASI BANTGENİŞLİĞİ PAYLAŞIMI

Yağcıoğlu, Mert

Doktora, Elektrik ve Bilgisayar Mühendisliği, Altınbaş Üniversitesi,

Danışman: Prof. Dr. Oğuz Bayat

Tarih: Temmuz, 2019

Sayfa Sayısı: 70

Son yıllarda telekomünikasyon sistemlerinde meydana gelen gelişmeler yeni taleplerin ortaya çıkmasına sebep olmuştur. Kablosuz haberleşme sistemi kullanıcıları için, veri aktarım hızı ve veri paylaşımı en önemli konular haline gelmiştir. Her geçen gün yaşanan teknolojik gelişmeler sayesinde veri aktarım hızı öngörülemeyen boyutlara ulaşmıştır. Kullanıcıların talepleri ve frekans spektrumundaki sınırlamalar göz önünde bulundurulduğunda, kaynak tahsisinin etkisi, kaynakların dağıtımı ve mevcut kaynakların etkin kullanımının önemini açıkça anlayabiliyoruz. Bununla birlikte, bilim insanları hücre içinde meydana gelen parazitlerden kaçınmak istiyorlar. Bu nedenle, LTE (Long term evolution – Uzun vadeli evrim) sistemlerinde kullanılan OFDMA (orthogonal frequency division multiple access - dikey frekans bölmeli çoklayıcı erişimi) yöntemi ile birbirlerine dik alt taşıyıcılar kullanarak hücre içi girişimleri en aza indirebilmektedir. Ancak, hücreler arası girişim, hücresel sistemlerin uydu yeri bağı (downlink) performanslarını sınırlamaktadır. Bu nedenle bu tezde, hücreler arası girişimi en aza indirgeyebilmek için kullanılan çeşitli girişim engelleyici teknikler analiz edilip karşılaştırılmıştır. Bu tekniklerden bir tanesi detaylı olarak incelenmiş ve incelenen bu teknikte birtakım iyileştirmeler yapılmıştır. Bu tekniğin ilk amacı, frekansın yeniden kullanımını sağlayan tekniği geliştirerek, hücreler arası etkileşimi en aza indirmektir. Ayrıca, tüm sistemin veri miktarını ve (SINR) sinyal parazit artı gürültü oranını arttırmayı ve bant genişliğini hücreler arasında dinamik olarak tahsis ederek ve yeniden konumlandırarak hücrelerin aşırı yüklenmesini önlemektir. Önerilen tekniğin son amacı ise, deneyim tabanlı paket planlayıcı olarak adlandırılan (EBPS) ve baz istasyonu planlayıcılarını optimize ederek kullanıcılar arasındaki adaleti sağlayan bir algoritma geliştirmektir. Tezimde yukarıda izah ettiğim amaçları

birleştirerek, deneyim tabanlı dinamik yumuşak yeniden frekans kullanımı (EB_{DSFR}) olarak adlandırılan algoritmayı önerdim. Öncelikli olarak, EB_{DSFR} tekniği Reuse-1, Reuse-3, Fractional Frequency Reuse (FFR), ve Soft Frequency Reuse (SFR) teknikleri karşılaştırılmıştır. Daha sonra, önerilen teknik, hücreler arası dinamik bant genişliği adil paylaşımlı (FFR_{DIBFS}) ve hücreler arası dinamik bant genişliği adil paylaşımlı Reuse-3 ($Reuse3_{DIBFS}$) yöntemler ile karşılaştırılmıştır.

Anahtar kelimeler: Frekansın yeniden kullanımı, Hücreler arası girişim koordinasyonu, LTE, OFDMA, Veri miktarı, SINR, Kapasite, Planlayıcı, Yük dengesi

ABSTRACT

EXPERIENCE BASED DYNAMIC INTER-CELLULAR BANDWIDTH SHARING FOR LTE OFDMA NETWORKS

Yağcıoğlu, Mert

PhD, Electric and Computer Engineering, Altınbaş University,

Supervisor: Prof. Oğuz Bayat

Date: July, 2019

Pages: 70

In recent years, developments in telecommunications systems have led to the appearance of new demands. For wireless communication systems users, data transmission speed and data sharing have become the most important issues. Thanks to the technological advancements that have been experienced every day, the data transmission speeds have reached unpredictable dimensions. When considering the users' demands and limitation of the frequency spectrum, it is clearly understood the importance of effective way of resource allocation, resources distribution and efficient use of existing resources. At the same time, scientists want to avoid intra-cell interference. For this reason, orthogonal frequency division multiple access (OFDMA) in Long Term Evolution (LTE) can minimize intra-cell interference using sub-carriers that are orthogonal to each other. But, inter-cell interference, limits the downlink performance of cellular systems. To minimize inter-cell interference, several interference cancellation techniques have been analyzed and compared. One of these techniques has been analyzed in detailed and some improvements made in this technique. The first objective of this technique is to minimize inter-cell interference by developing the frequency reuse technique. Also, it aims to increase the throughput and signal to interference plus noise ratio (SINR) of the entire setup and prevents the overload of the cells by allocating and reallocating the bandwidth dynamically between the cells. The last target of the proposed technique is to progress a fairness scheduler algorithm among users by optimizing the base station schedulers that is called experience-based packet scheduler (EBPS). Finally, combining all these targets, I proposed the algorithm called Experiment Based Dynamic Soft Frequency Reuse (EB_{DSFR}) in this thesis. First of all, EB_{DSFR} technique has been compared with Reuse-1, Reuse-3, Fractional Frequency Reuse (FFR), and Soft Frequency Reuse (SFR). Secondly, I compared our proposed technique with the Dynamic Inter-cellular Bandwidth Fair Sharing FFR (FFR_{DIBFS}) and Dynamic Inter-cellular Bandwidth Fair Sharing Reuse-3 ($Reuse3_{DIBFS}$).

Keywords: Frequency Reuse, Inter-Cell Interference Coordination, LTE, OFDMA, Throughput, SINR, Capacity, Scheduling, Load Balancing

TABLE OF CONTENTS

Pages

LIST OF FIGURES

Pages

LIST OF TABLES

Pages

ABBREVIATIONS

QoE	:	Quality of Experience
ICI	:	Inter-Cell Interference
ISI	:	Inter symbol interference
CCI	:	Co-Channel interference
QoS	:	Quality of Service
FFR	:	Fractional Frequency Reuse
UE	:	User Equipment
RB	:	Resource Block
BS	:	Base Station
UL	:	Uplink
DL	:	Downlink
FRF	:	Frequency Reuse Factor
CCU	:	Cell Center Users
CEU	:	Cell Edge Users
SFR	:	Soft Frequency Reuse
UFR	:	Universal Frequency Reuse
ICIC	:	Inter-cell Interference Coordination
SINR	:	Signal to Interference Noise Ratio
RCAC:		Radius of Central Area of Cell
BAC	:	Boundary Area of Cell
RRM	:	Radio Resource Management
PFR	:	Partial Frequency Reuse
OFDM	:	Orthogonal Frequency Division Multiplexing
OFDMA	:	Orthogonal Frequency Division Multiple Access
RAN	:	Radio Access Network
RAT	:	Radio Access Technology
RRM	:	Radio Resource Management
SC-FDMA	:	Single Carrier Frequency Division Multiple Access
SINR	:	Signal to Interference Plus Noise Ratio
TTI	:	Transmit Time Interval
UMTS	:	Universal Mobile Terrestrial radio access System

1. INTRODUCTION

Long Term Evolution (LTE) uses Orthogonal Frequency Division Multiple Access (OFDMA) [1][2] that is a multi-user version of the Orthogonal Frequency Division Multiplexing (OFDM) digital modulation scheme to avoid the intra-cell interference. OFDMA provides better spectral efficiency and effective use of bandwidth [53]. In OFDMA system data is delivered on a huge number of parallel narrow-band subcarriers [46]. Also, Resource Block (RB) is the smallest unit of resources that can be allocated to a user [3]. The resource block is 180 kHz wide in frequency and 1 slot long in time.

Because of the orthogonality, intra-cell interference is removed. But, there is an important issue that is called Inter-Cell Interference (ICI) [4] for the cellular networks. This allows simultaneous low data rate transmission for the different users. Also, the bandwidth is limited for cellular systems so, the available spectrum should be used more efficiently. The cell edge users are affected from the interference of neighboring cells especially the cells that use same frequency with the serving cell. For this reason, overall cell performance decreases and SINR can be lower. To avoid this problem inter-cell interference coordination (ICIC) [5], [6] strategy can be used. This provides better performance [50] of the cellular system and minimize the interference.

Reuse-N, Fractional Frequency Reuse (FFR) [7], and Soft Frequency Reuse (SFR) [8],[9] are the main ICIC techniques that can mitigate the inter-cell interference. According to Reuse-1 approach, all the cells use same frequency band and it provides high system capacity and spectrum efficiency. However, it is not a solution for the ICI problem. To solve the ICI problem Reuse-N has been proposed. In this technique, neighboring cells have different frequency band in a cluster (group of cells). But, in Reuse-N there is a difficulty for the use of available bandwidth. To protect the users especially located in the cell edges from the ICI, Fractional Frequency Reuse (FFR) technique is proposed. Each cell is divided in two frequency band zones that are cell center (inner cell) zone and cell edge (outer cell) zone. In the cell center zone frequency Reuse-1 method is used and in the cell edge zone frequency reuse-n method is used. Finally, Soft Frequency Reuse (SFR) [10], [26] technique has been managed to improve both systems performance and spectral efficiency. Like FFR, SFR use two frequency band zones, cell center end cell edge. But, difference is that, SFR uses all the available spectrum in each cell when reducing the inter-cell interference. The restriction is on the power allocation [40].

In multi-cellular scenarios, many users aim to share limited amount of data at the same time. These resources are shared between the users by using Multi-Carrier dynamic scheduling systems. Dynamic scheduling refers to the calculation of how physical layer resources are allocated to each cell and each user in each given time slots (Time Transmission Interval) and how the whole system can be optimized [11]. Sometimes, this seems to be a very complicated problem, because it is necessary to consider different variables such as, channel load condition, SINR or the user quality of service (QoS). So, resource allocation [42] (subcarrier allocation) should be optimized by considering these variables. In this thesis, I also added another scheduling scheme that supply allocating and reallocating the bandwidth to the cells. In some case the traffic conditions of the cells can be disordered, and some cells may be overloaded. In these situations, our dynamic scheduling selects the cell that has the highest density as a receiver cell and supply the resource blocks from the cell that has lowest density (donor cell). These cells are in the same cluster and every time slots donor and receiver cells are calculated. Because of this dynamic scheduling, throughput rates are increased based on the user and total system.

Finally, I proposed one more scheduling scheme based on the user fairness that is called Experience Based Packet Scheduler (EBPS) [13], [34]. This scheduler optimizes resources transmission to the users by considering at multiple criteria by using Multi-Carrier modulation. The criteria include users' previous experience, base station load, real-time channel quality and user subscription class. The above-mentioned previous experience is formulized under the experience classifier ($EC_u(n)$) and it is calculated by using user's previous call success rate ($CSR_u(n)$), the average throughput rate ($Rp_u(n)$), and bit error rate ($BER_u(n)$). All these data are collected to create the decision metric $EBPS_u(n)$. The system aims to provide more throughput per unit time to the high-class users. The dynamic packet scheduler also eliminates unjust treatment by providing fairness to the users. All the data transmissions are distributed according to LTE technology [21]. All the algorithms are combined, and I tried to increase overall system capacity and throughput fairness among users.

This thesis is organized as follows. In Section II, I describe the Inter-cell interference coordination techniques in detailed. In Section III, I give the description system model of the LTE downlink and method of throughput estimation. Our proposed algorithm is described in this section. Dynamic resource allocation and EBPS algorithm are explained detailly. In Section IV, simulation result and analysis are shown in this section. Finally, in Section V, I concluded our study and present our final remark along with the future work.

2. ORTHOGONAL FREQUENCY DIVISION MULTIPLE ACCESS

Orthogonal frequency-division multiple access (OFDMA) is a technique used to receive and transmit radio signals in LTE that can do the same tasks as any other technique of its kind and that enables simultaneous communication between the base station and multiple mobiles. It is also a powerful way of minimizing fading and inter-symbol interference, which we will mention in next part of this thesis. Other communication systems also incorporate OFDMA. These include wireless local area networks (IEEE 802.11 versions a, g and n), WiMAX (IEEE 802.16) and digital television and radio broadcasting [38]. Here, I will deal with the fundamentals of OFDMA and demonstrate its application to a mobile network. In addition, I will talk about single carrier frequency-division multiple access (SC-FDMA), a modified radio transmission technique used for LTE uplink. Unlike in OFDMA, LTE is the first to utilize SC-FDMA.

2.1 ORTHOGONAL FREQUENCY DIVISION MULTIPLEXING

2.1.1 Reduction of Inter-Symbol Interference Using OFDM

In this thesis, I demonstrate how transmitting data at a high rate in a multipath environment causes inter symbol interference (ISI). For instance, let's say delay spread is 1 μs and data rate is 400 ksps, this can cause the symbols to be overlapped by 40% at the receiver and lead to interference and bit errors. Orthogonal frequency-division multiplexing (OFDM) is an efficient method of solving these errors. OFDM transmitters divide the data into a number of parallel sub-streams and send them all over varying frequencies (sub-carriers). If the total rate of sending data is unchanged, sub-carriers start to get lesser rate, lengthening the symbol duration and reducing the ISI along with the error rate.

Figure 2.1 shows a simple example of this where I supposed that I divided the original data stream into four sub-carriers with frequencies $f1$-$f4$. The data rate on each sub-carrier has become 100 ksps, increasing the symbol duration to 10 μs. In the case that the delay spread remains at 1 μs, the symbols will have overlapped only by 10%. This can help reduce ISI to one quarter of the previous amount while also reducing errors. Practically, LTE is able to incorporate sub-carriers in significant quantities (up to 1200 in Release 8) and reduce ISI to insignificant levels.

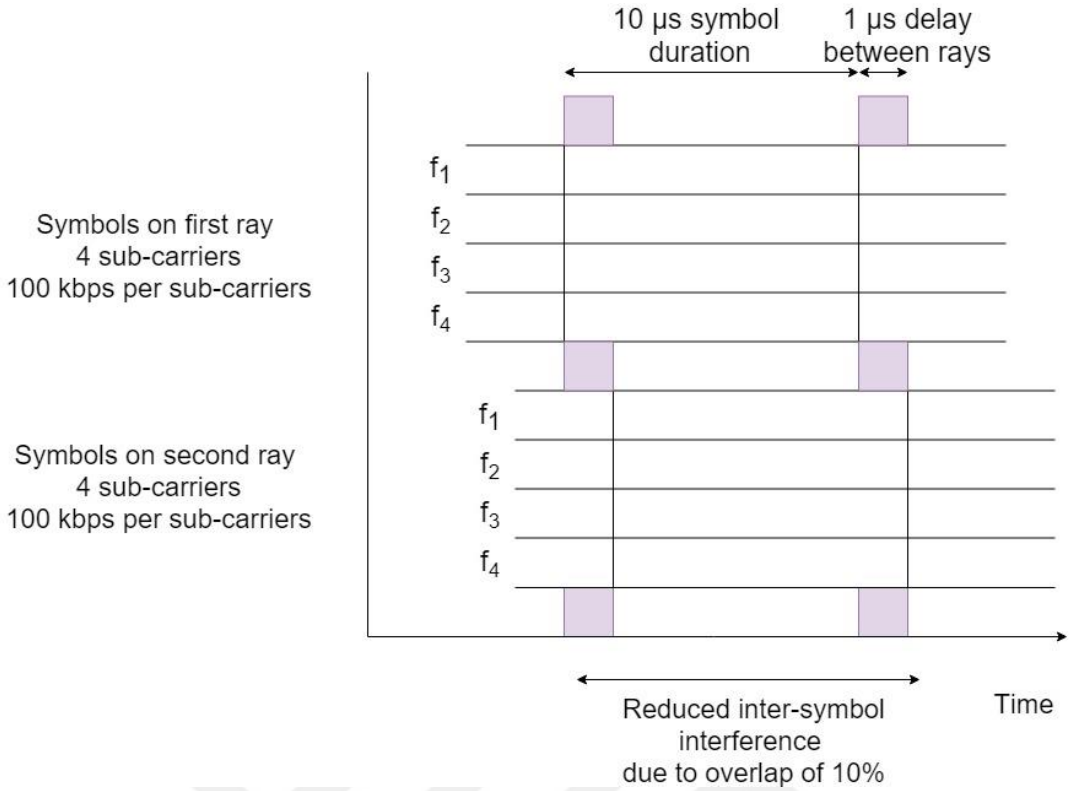

Figure 2.1: Reduction of inter-symbol interference by transmission on multiple sub-carriers.

2.1.2 The OFDM Transmitter

Figure 2.2 shows an analogue OFDM transmitter along with certain simplified data that I will talk about in due time. However, the fundamentals can be clearly observed here.

A bitstream coming from higher layer protocols are accepted, then converted into symbols via the selected modulation [e.g.: quadrature phase shift keying (QPSK)]. Afterwards, the serial-to-parallel converter picks up a number of symbols equal to the number of sub-carriers (4 in this instance) and adjusts the amplitude and phase of each sub-carrier to mix them with a symbol.

The sub-carrier spacing used by LTE is fixed at 15 kHz. The frequencies of the sub-carriers in Figure 2.2 are 0, 15, 30 and 45 kHz which I will eventually rearrange to radio frequency (RF), where symbol duration corresponds to sub-carrier spacing (approximately 66.7 µs). This is completely optional here; however, why I chose it will become clear at the proper time. Accordingly, for the symbol duration, the 15, 30 and 45 kHz sub-carriers undergo one (66.7 µs), two and three cycles, respectively.

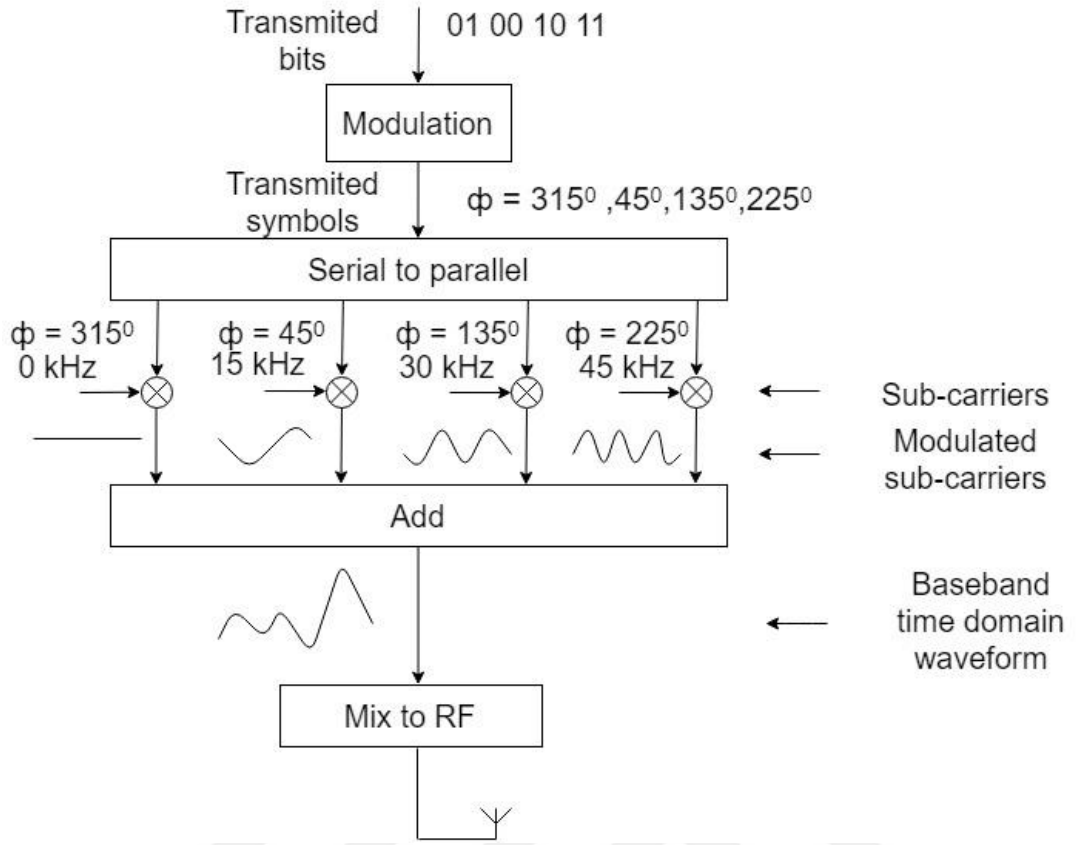

Figure 2.2: Processing steps in a simplified analogue OFDM transmitter.

The four sine waves (0, 15, 30 and 45 kHz) have amplitudes and phases representing the eight bits. A single time-domain waveform can be generated by adding these four together. This time-domain waveform is the representation of the signal that we need to send at a low frequency. What remains is to rearrange the waveform to RF for transmission.

Figure 2.3 involves 3 extensions. First, I add four more sub-carriers at −15, −30, −45 and −60 kHz, all at negative frequencies, to be transmitted below the carrier frequency. For instance, the 15 kHz sub-carrier gets 800.015 MHz for 800 MHz carrier frequency, and its negative counterpart (−15 kHz) gets 799.985 MHz.

Next, I separate the sub-carriers according to positive and negative frequencies. This is done by maintaining the in-phase and quadrature portions of the sub-carriers for a majority of the transmission process. In the example in Figure 2.3, the 15 kHz and −15 kHz signals have the same in-phase components; however, they are distinguishable due to their different quadrature components. This rearrangement results in all positive frequencies. The quadrature components may then be ignored.

Third, digital processing is a lot more appealing than analogue processing. In the example in Figure 2.3, the components are sampled 8 times for each symbol. This enables the sampling of the −60 kHz sub-carrier twice per cycle. Usually, the minimum number of samples for each symbol equals the total number of sub-carriers. This enables digital operations of mixing and addition, leading to a digital time-domain waveform containing all the information needed. Now, I can transform the digital waveform into analogue and filter and rearrange it to RF.

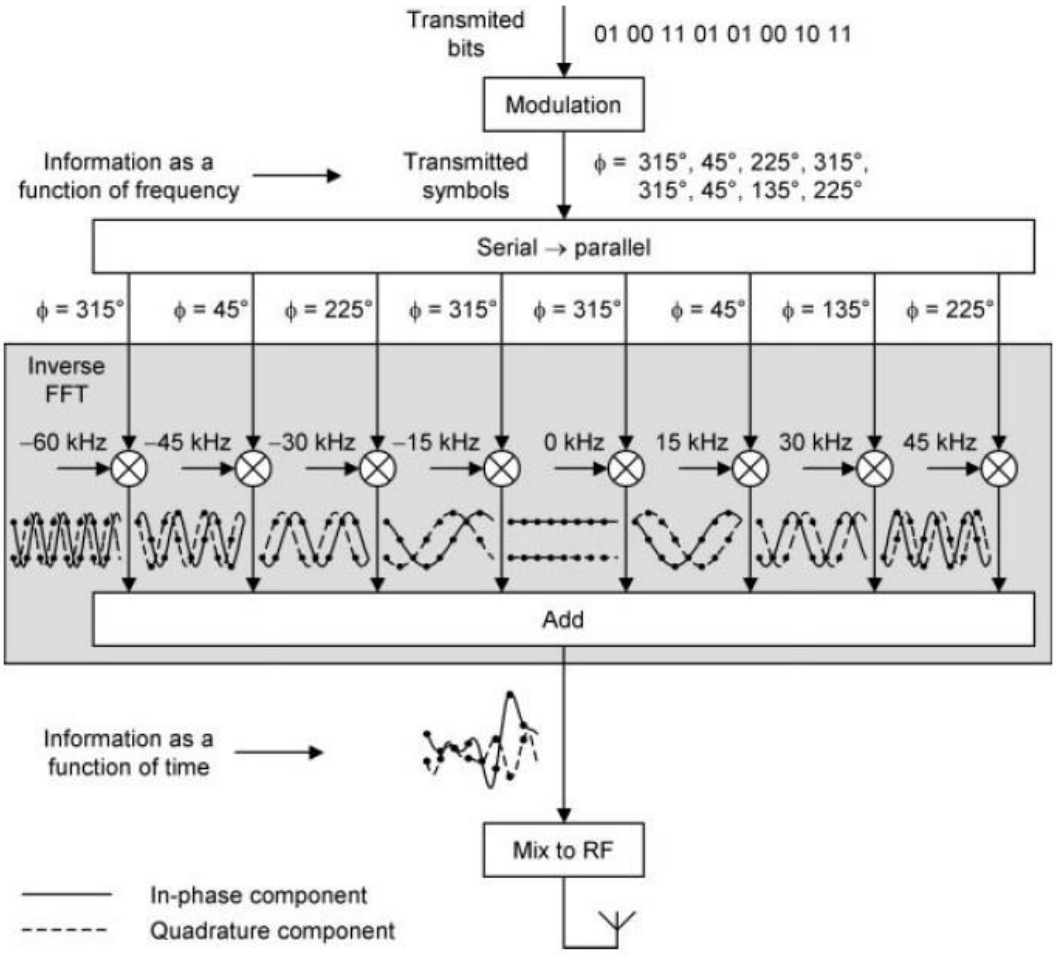

Figure 2.3: Processing steps in a digital OFDM transmitter.

There are two key elements in the sequence that I will not deal with. When converting from serial to parallel, the data stands for the amplitude and phase of the sub-carriers as a function of frequency. Towards the end, following the addition, it stands for both components of the signal as a function of time. It can be observed that rearrangement and addition have transformed the data into the latter.

This is named the inverse discrete Fourier transform (DFT), a popular computational technique. Normal Fourier transform does the opposite, turning to data into a function of frequency. This technique negates the necessity for the rearrangement in Figures 2.2 and 2.3, allowing us to put the symbols through DFT and simply obtain the time-domain signal.

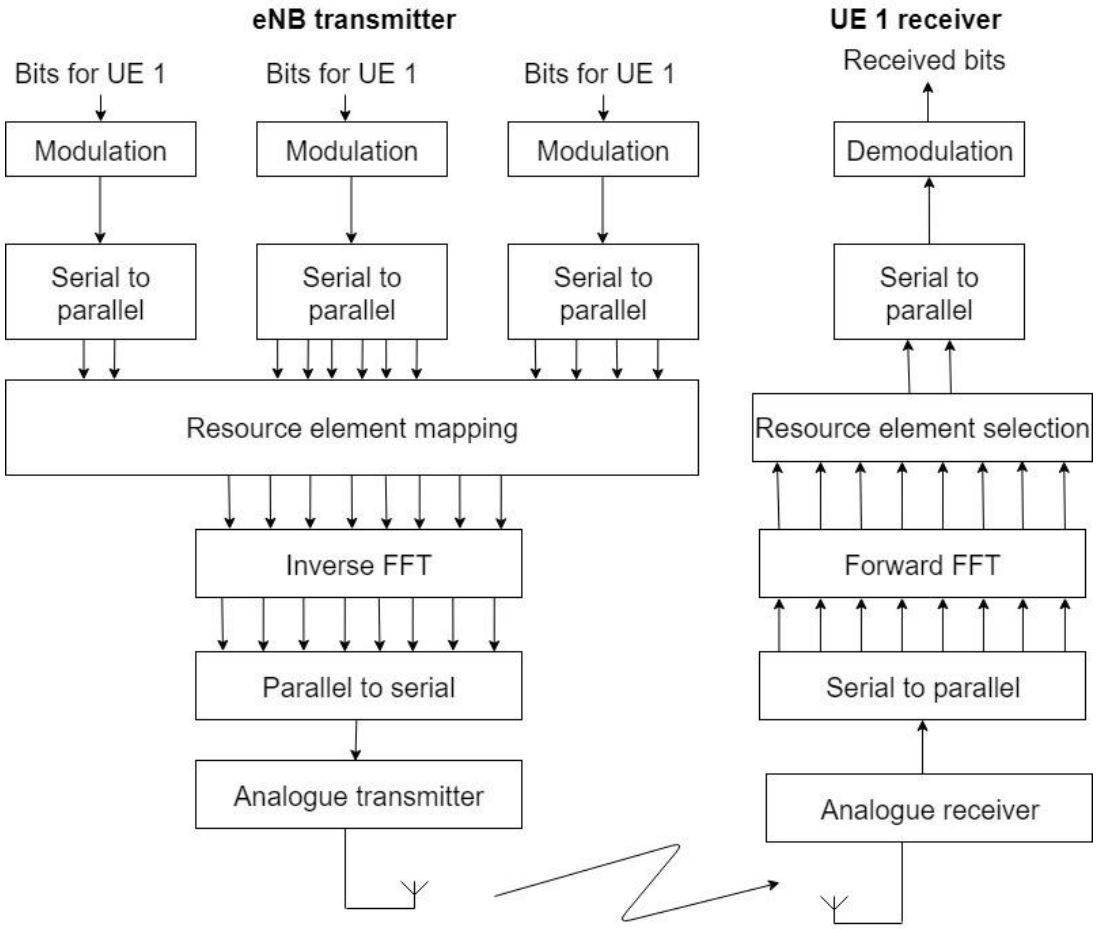

Figure 2.4: Initial block diagram of an OFDM transmitter and receiver.

Similarly, the discrete FT may be used much faster with the fast Fourier transform (FFT) algorithm. Using this algorithm allows a computationally efficient use of the transmitter and receiver by limiting the computational load on them. One significant restriction is that the quantity of data points needs to be equal to a power of two or be a product of only small prime numbers for the efficient use of FFT. [36] and [37] explain the Fourier transform in greater detail.

2.1.3 Initial Block Diagram

Figure 2.4 shows an OFDM transmitter and receiver with the use of all the above-mentioned principles. With the assumption that the system operates on the downlink, the transmitter should

be in the base station, and the receiver in the mobile station. There are also some simplified data here that I will clarify shortly.

In Figure 2.4, the base station sends bitstreams to 3 mobiles and arranges each one independently. This is likely done using different modulations. Afterwards, the symbol streams are put through a serial-to-parallel converter and divided into sub-streams. Here, the data rate determines the number of sub-streams for each mobile (e.g.: many more sub-streams for a video application compared to a voice application). The resource element mapper selects which individual sub-stream to transit on which sub-carrier. In the case of a mobile, the sub-carriers may be divided (mobile 2) or be in one contiguous block (mobiles 1 and 3). The information obtained here represents the amplitudes and phases of the sub-carriers as a function of frequency. I can now obtain their in-phase and quadrature components for the time-domain waveform by passing them through the inverse FFT, enabling us to digitize, filter and rearrange them to RF.

The process is reversed in the mobile, as in that it samples the signal, filters it and converts it down to baseband. Accordingly, the data undergo a forward FFT, and the amplitudes and phases of the sub-carriers are acquired. Here, I make the assumption that the mobile has obtained from the base station the information regarding which sub-carriers to use. The mobile uses this information to select the needed sub-carriers, obtain the transmitted information and discard the remaining ones.

2.2 OFDMA IN A MOBILE CELLULAR NETWORK

2.2.1 Multiple Access

In Figure 2.4, the base station uses orthogonal frequency-division multiplexing and transmits to three mobiles simultaneously. I can have the resources shared dynamically between all mobiles and take this idea to the next step. This is called orthogonal frequency-division multiple access (OFDMA) (Figure 2.5).

In OFDMA, the base station aims to meet the needs of separate applications and thus shares the resources by transmitting to mobiles at different times and frequencies [44]. For example, mobile 1 receives a voice over IP (VoIP) stream. Therefore, the data rate (equal to the quantity of sub-carriers, as discussed above) must be low but constant. However, mobile 2 receives a stream of non-real time packet data, which means higher average data rate, albeit in bursts, resulting in a varying number of sub-carriers.

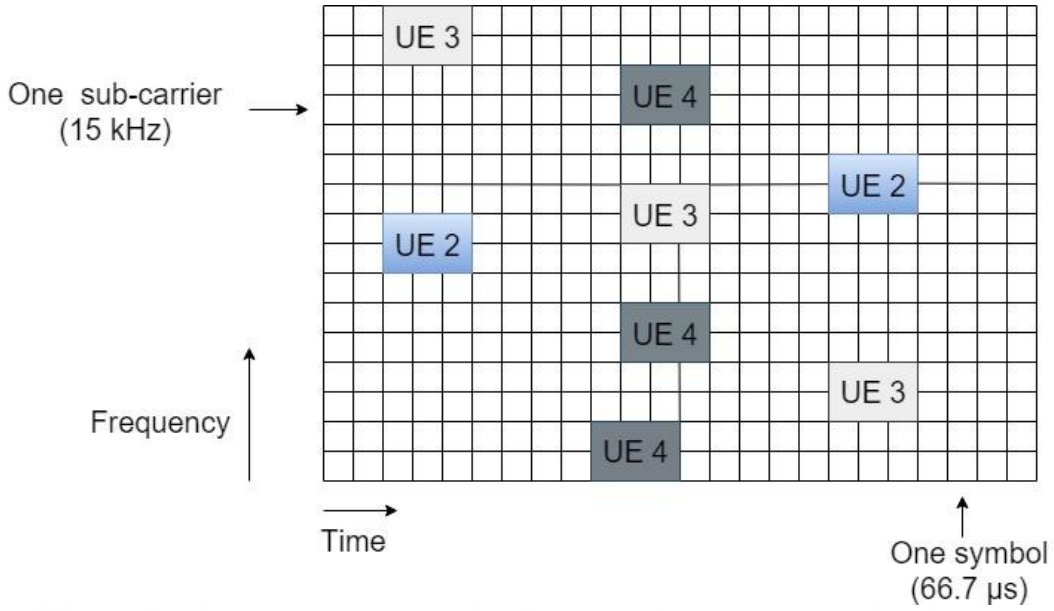

Figure 2.5: Implementation of time and frequency division multiple access when using OFDMA.

The base station is able to respond to frequency-dependent fading by distributing sub-carriers where the mobile gets a strong signal, as in the example where mobile 3 gets a VoIP stream, while under effect by frequency-dependent fading. In turn, the base station distributes the sub-carriers accordingly and changes this distribution in accordance with the fading pattern. Similarly, it is able transmit to mobile 4 through two groups of sub-carriers distinguished by a fade.

Using the aforementioned change of distribution in accordance with the fading pattern, OFDMA transmitters are able to reduce the impact of time-dependent fading and frequency-dependent fading by a great margin.

2.2.2 Fractional Frequency Re-Use

The aforementioned techniques allow a single base station to transmit to many mobiles. However, this rises the potential problem of interference, where every mobile will need to receive from one base station, as mobile communication systems normally have many base stations. The interference needs to be minimized for the mobile to get successful reception.

There have been two different techniques used for this purpose. In GSM, nearby cells use various carrier frequencies to transmit, where cells may use one fourth of the bandwidth each, resulting in a 25% re-use factor. While reducing the interference among close cells, this calls for an inefficient use of the frequency band. UMTS has a 100% re-use factor, where the cells

have equal carrier frequency. This results in a more efficient use of the frequency band, while also increasing interference.

LTE networks allow base stations to send information in the same frequency band, but they can distribute the sub-carriers in the same band flexibly via the fractional frequency re-use technique.

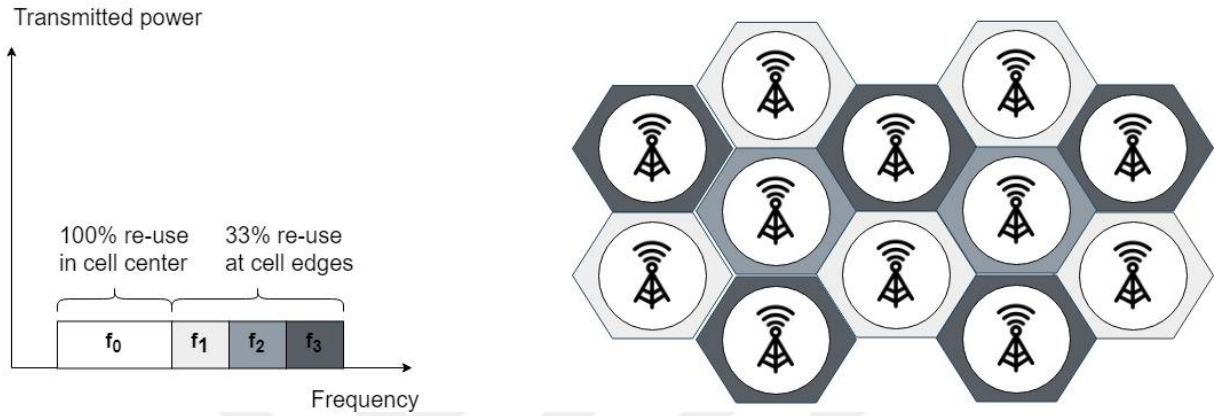

Figure 2.6: Example implementation of fractional frequency re-use when using OFDMA. (a) Use of the frequency domain. (b) Resulting network plan.

Figure 2.6 is a simple example of this, where each base station controls a cell, and all cells share the same frequency band. Within the same band, cells use the same set of sub-carriers, denoted *f*0, and transmit to nearby mobiles. This is beneficial as each mobile is close to its base station, keeping reception enough to overwhelm. Interference easily damages farther mobiles due to their less powerful signals. This can be avoided by having neighboring cells transmit to the mobiles in question via other sets of sub-carriers. In Figure 2.6, half of the frequency band is set apart for close mobiles, while the other half is separated into 3 sets denoted as *f*1, *f*2 and *f*3 for distant mobiles, resulting in a 67% re-use factor.

More changeable incorporations can be achieved where, for instance, one cell uses a set for farther mobiles, and the neighboring cells use the same for closer ones. This can be further supported by having base stations send and receive signaling messages over the X2 interface. These messages would tell each other about their usage of the frequency band.

2.2.3 Channel Estimation

Figure 2.7 is similar to the previous one, albeit with 2 additional processes. The first is channel estimation and equalization, while the second constitutes the insertion of a cyclic prefix into the data stream by the transmitter to be later excluded.

As for channel estimation, each sub-carrier can reach the receiver with an optional amplitude and phase. This is negated by the OFDMA transmitter injecting reference symbols into the transmitted data stream, which are measured by the receiver and compared with the transmitted symbols. The receiver then uses the result of this comparison to remove the amplitude changes and phase shifts from the coming signal.

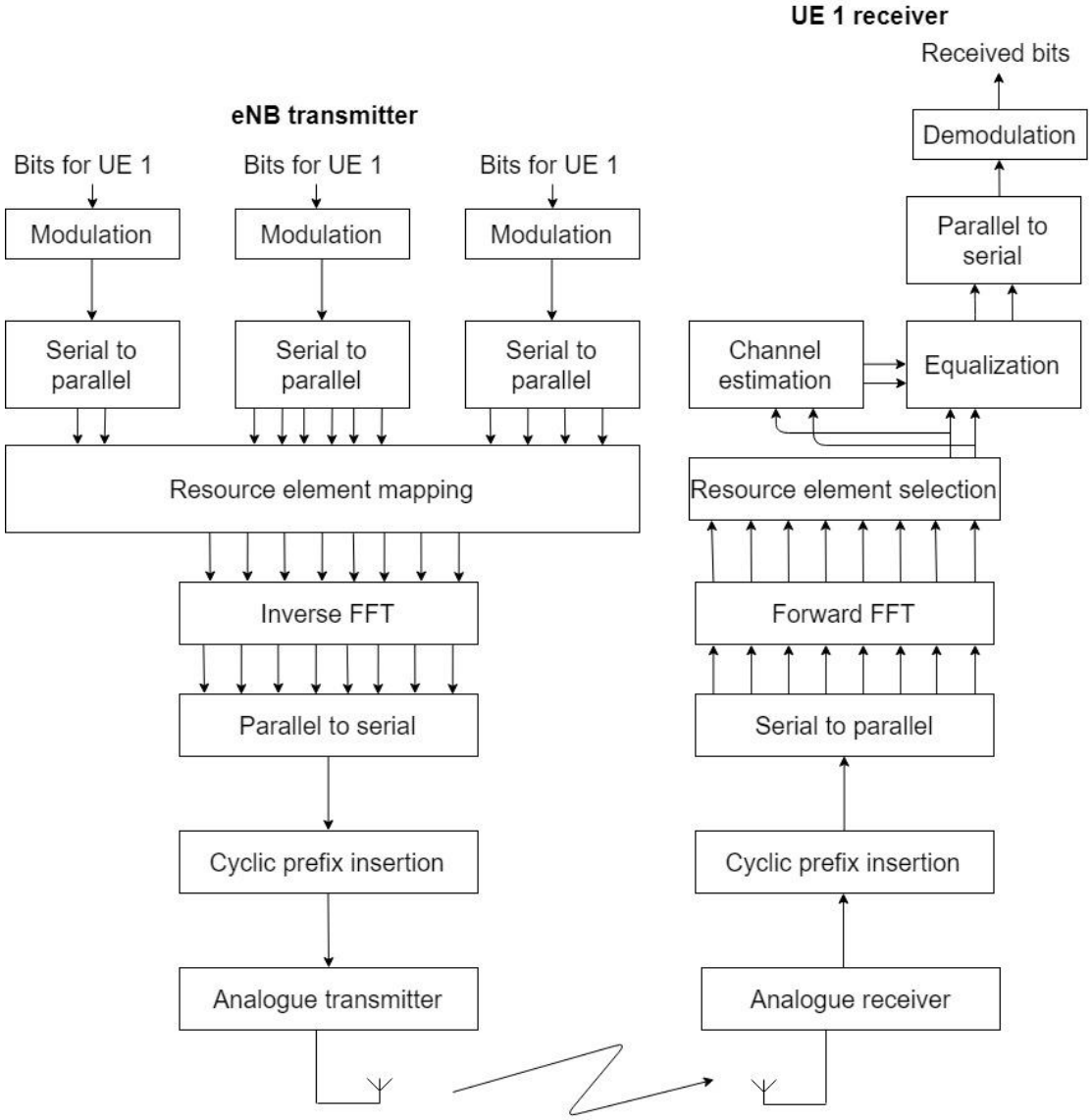

Figure 2.7: Complete block diagram of an OFDMA transmitter and receiver.

For frequency-dependent fading, amplitude and phase variances are functions of both frequency and time. These changes affect sub-carriers in various ways, where it needs to be ensured that the receiver measures all the needed information. For this reason, the reference symbols are dispersed across both domains. The reference symbols do not cause an important overhead as they constitute up to approximately 10% of the data stream.

2.2.4 Cyclic Prefix Insertion

I demonstrated in previous parts how OFDMA reduces ISI by transmitting data on multiple sub-carriers, and I will be able to eliminate ISI completely with a final technique.

The idea here is to add a guard period (GP), where no transmit is done, before each symbol. As long as the guard period outlasts the delay spread, the receiver will be able to read data from each symbol one by one. This will negate possible overlaps with the symbols that come before or after. However, this will naturally result in some confusion as the symbols will reach the receiver at different times and on different rays, leading to the need of some extra processing, which is, however, relatively straightforward.

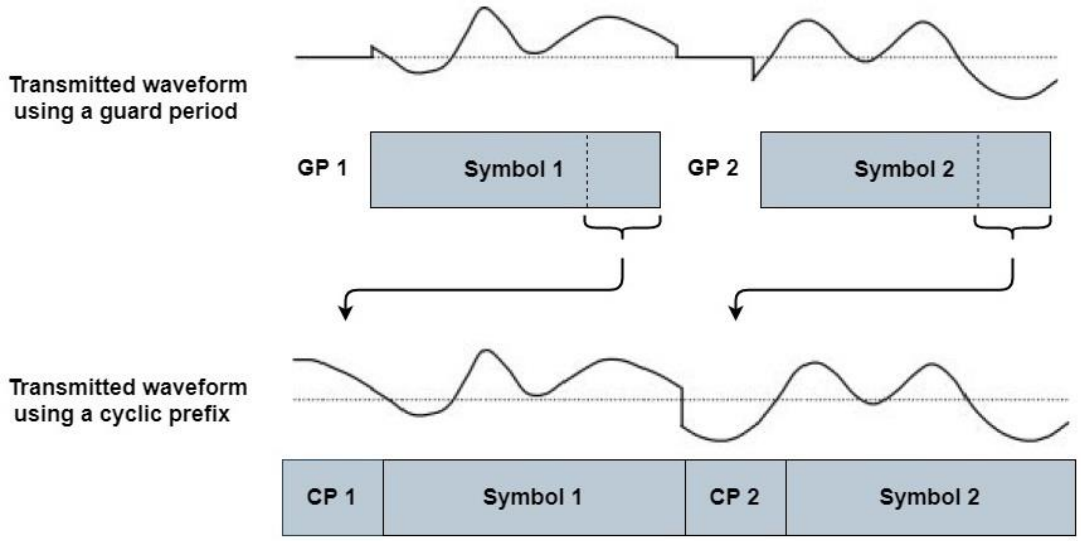

Figure 2.8: Operation of cyclic prefix insertion.

LTE utilizes cyclic prefix (CP) insertion shown in Figure 2.8. In this mildly more complicated technique, the transmitter adds a GP before each symbol but proceeds to copy the information from the end of the following symbol to complete the GP. In case the cyclic prefix outlasts the delay spread, the receiver will again be able to read data from each symbol one by one.

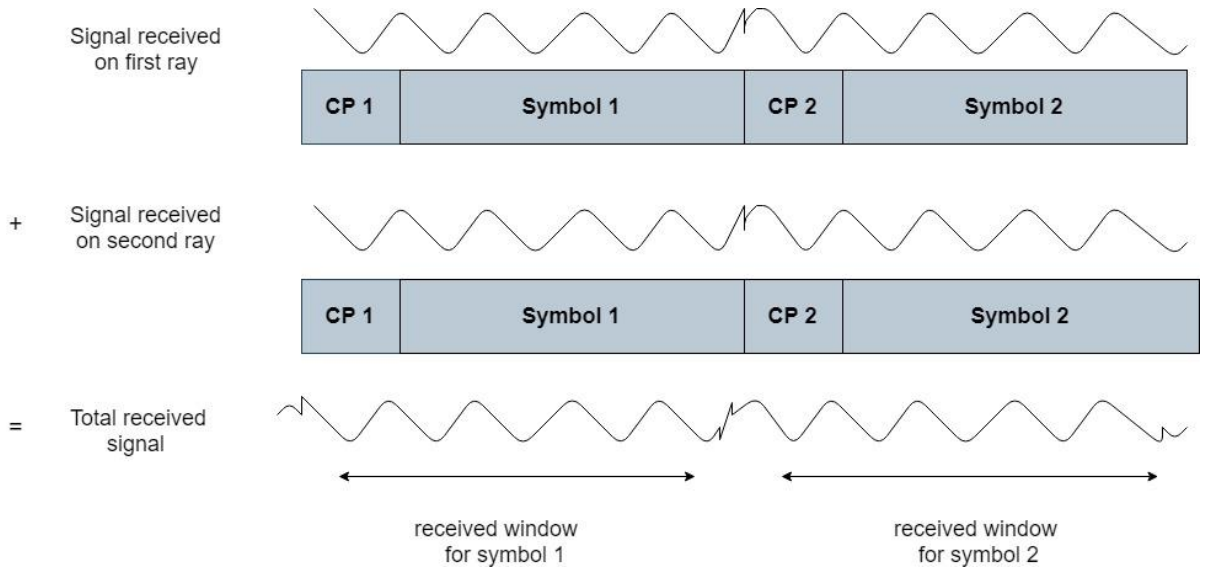

Figure 2.9: Operation of the cyclic prefix on a single sub-carrier.

Looking at one sub-carrier will show us how cyclic prefix insertion works (Figure 2.9). The transmitted signal is a sine wave. Its amplitude and phase differ with each symbol, which comprise the precise amount of cycles of the sine wave. This results in equal amplitudes and phases at the start and end of each symbol, leading to a smooth change of the transmission progressing from one cyclic prefix to the next symbol.

For multipath environments, multiple copies of the transmitted signal are picked up by the receiver, along with multiple arrival times, which accumulate at the receiver. This gives a sine wave with equal frequency and distinct amplitude and phase, not disturbing the smooth change mentioned earlier. However, a few glitches might still be encountered at the beginning of the cyclic prefix and the end of the symbol, the locations involving interference of the symbols before and after.

The receiver handles the coming signal in a window and discards all else. This window has equal length with that of the symbol duration, and as long as it is placed correctly, the received signal will be exactly what was transmitted, with no glitches. The signal undergoes an amplitude change and a phase shift and nothing else. However, the receiver is able to compensate for the change and shift through the channel estimation and equalization techniques we previously mentioned. Thus, the cyclic prefix can be handled with no extra processing.

While the system does use multiple sub-carriers, it has been established that these do not interfere with each other and can be processed independently. Hence, this is not a downside.

Normally, the cyclic prefix used by LTE is approximately 4.7 μs. This means up to approximately 1.4 km path difference from the longest rays to the shortest ones. This is sufficient for all cells, with the exception of the biggest and most organized ones. The cyclic prefix decreases the data rate by approximately 7%, which is worth the negation of ISI.

2.2.5 Use of the Frequency Domain

I will now handle the way mobile communication systems use the frequency domain in more detail. In case of interference in a traditional analogue FDMA, mobiles need to measure the signal on one sub-carrier. To minimize interference, they need to be divided by wide guard bands, which suggests inefficient use of the frequency domain.

Considering the same situation with OFDMA, sub-carriers start as a sine wave; however, their amplitude and phase are changed by the modulation process at intervals of the symbol duration *T*, equal to 66.7 μs. This enlarges the signal in the frequency domain to approximately T^{-1} bandwidth (see Figure 2.10 for more). Here, the amplitudes of the sub-carriers oscillate both sides of zero and cross it at regular T^{-1} interval [this may be recognized as a sinc function $(x^{-1} \sin x)$].

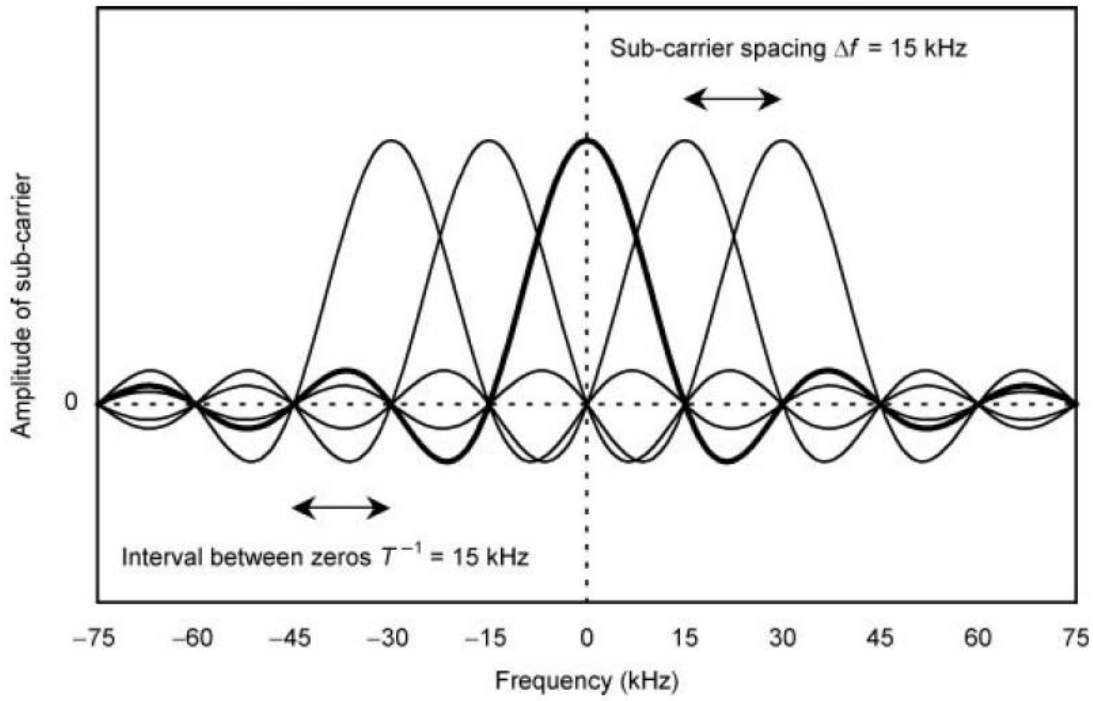

Figure 2.10: Amplitudes of the signals transmitted on neighboring sub-carriers, as a function of frequency.

The interval between adjacent sub-carriers is the sub-carrier spacing Δf. In the case that $\Delta f = T^{-1}$, they overlap; however, the peak return of one collides with the zeros of the others. Consequently, the mobile can acquire one sub-carrier and measure its amplitude and phase with zero interference, even though they might be tightly cluttered (these are suggested to be orthogonal).

This yields a very efficient use of the frequency domain and is one of the reasons why LTE has a much greater spectral efficiency compared to the prior systems. In addition, it legitimizes the selection in Section 2.1.2, where I adjusted the symbol duration T to be equal to that corresponding the spacing Δf.

2.2.6 Choice of Sub-Carrier Spacing

The previous suggestion works well for stationary mobiles. If otherwise, however, incoming rays are Doppler shifted to higher or lower frequencies, as will be the case for OFDMA sub-carriers.

For multipath environments, mobiles may move towards those that are shifted to higher frequencies and distance those shifted to lower frequencies. Consequently, the sub-carriers are not shifted but are instead clouded over an area of frequencies. Now, measuring the peak return of one sub-carrier will get interference from all else, resulting in the loss of the orthogonality property mentioned earlier.

As the Doppler shift is smaller compared to the sub-carrier spacing, there will still be an acceptable amount of interference [41]. Therefore, the sub-carrier spacing Δf needs to be chosen as follows:

$$\Delta f >> f_D \tag{2.1}$$

where f_D is the Doppler shift in Equation 2.2.

$$f_D = \frac{v}{c} f_c \tag{2.2}$$

where f_C is the carrier frequency, v is the speed of the mobile and c is the speed of light (3×10^8 ms^{-1}).

By design, LTE can worth with up to 350 km hr^{-1} mobile speed and up to approximately 3.5 GHz carrier frequency. This yields a Doppler shift up to approximately 1.1 kHz, which constitutes 7% of the sub-carrier spacing, negating the limitation mentioned before.

Another limitation on the parameters is that in order to minimize the effect of ISI, the symbol duration T needs to be chosen as follows:

$$T >> \tau \tag{2.3}$$

where τ is the delay spread of the radio channel, which is the difference between the arrival times of the earliest and latest rays. It can be calculated as follows:

$$\tau = \frac{\Delta L}{c} \tag{2.4}$$

where Δ_L is the difference between the path lengths of the longest and shortest rays.

As previously mentioned, LTE usually works with a maximum delay spread of approximately 4.7 μs, constituting 7% of the 66.7 μs symbol duration, which negates the second limitation.

In conclusion, in the case that the sub-carrier spacing is well below 15 kHz, the system will be inclined to interference between the sub-carriers at high mobile speeds. In the case that it is above it, the system will be inclined to interference between symbols in the bigger and more organized cells. The sub-carrier spacing we chose offers the best of both worlds among these two choices.

3. INTER-CELL INTERFERENCE COORDINATION (ICIC) TECHNIQUES

In this section, I described the Inter-Cell Interference Coordination (ICIC) techniques more comprehensively and especially Soft Frequency Reuse (SFR) [23] technique that I used our proposed algorithm. In multi cellular system the main problem is interference [35]. For the wireless systems available bandwidth is limited and this available bandwidth is wanted to use more efficiently. Overall system capacity should be increased, and all the spectrum should be used. For this reason, some frequency reuse and fraction methods are designed. But, some of these methods increase the co-channel interference [22] and some of them decrease the usage of available bandwidth.

3.1 REUSE-1 METHOD

Reuse-1 is the most popular technique for the use of overall bandwidth [12]. In Reuse-1 technique all the cells use same frequency band in a cluster with equal power. According to this approach, system capacity will be higher, and spectrum will be used more efficiently. However, this approach cannot solve the main interference problem. Because adjacent cells must use different frequency. It causes lower SINR especially for the cell edge users. Thus, users have lower throughput rate, and this affects overall system performance. In figure 3.1, we can see that; all cells use same frequency and equal power.

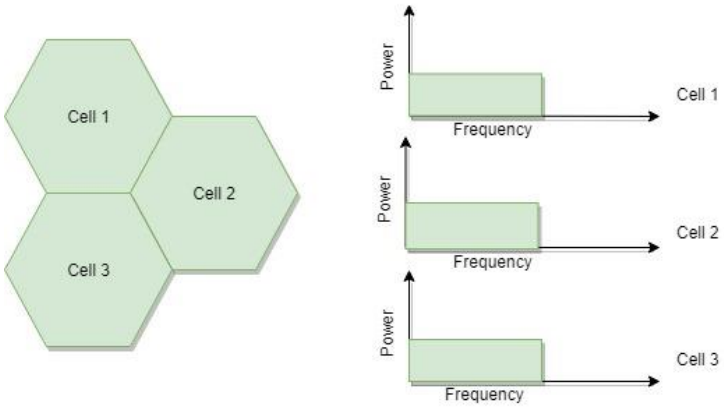

Figure 3.1: Frequency Reuse-1 Approach.

3.2 REUSE-3 METHOD

In order to solve the ICI problem [27] Reuse-3 has been proposed. In this technique, neighboring cells have different frequency band in a cluster (group of cells) so, cell edge users don't face

with the low SINR and power problems. But, in the Reuse-3 the main problem is that; every cell uses limited bandwidth. The frequency band is divided into 3 equal part and resources are allocated to three different groups. For example; I supposed that, there are seven cells in one cluster and according to Reuse-3, 1/3 of the available spectrum can be allocated to each cell. This means that, lower system capacity can be used, and available spectrum cannot be used efficiently. Although, users have good SINR level, the overall system capacity can be lower because of the less allocated resources. In figure 3.2, we can see that; all adjacent cells use distinct frequency and total bandwidth is 1/3. As the reuse factor increases, ICI will be decrease, at the same time each cell can use part of the bandwidth [11] [12].

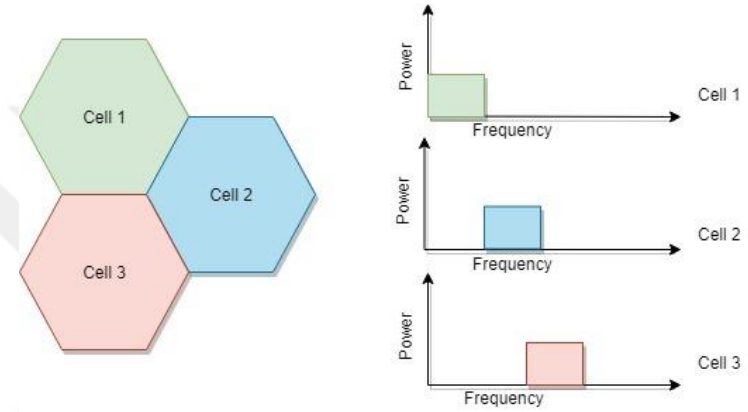

Figure 3.2: Frequency Reuse-3 Approach.

3.3 FRACTIONAL FREQUENCY REUSE (FFR) METHOD

To protect the cell edge users from the ICI [20] [28], Fractional Frequency Reuse (FFR) technique is proposed. Each cell is divided in two frequency band zones that are cell center zone and cell edge zone. In the cell center zone frequency Reuse-1 method is used and in the cell edge zone frequency Reuse-3 method is used.

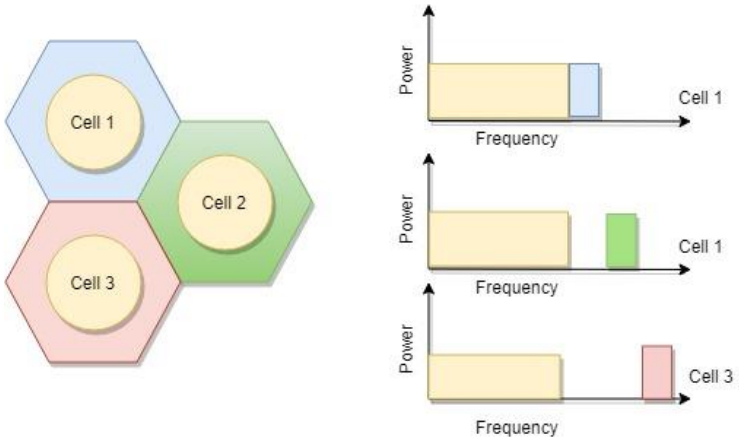

Figure 3.3: Fractional Frequency Reuse (FFR) Approach.

The advantages of the FFR is that, cell edge [39] users are served disjoint spectrum so, they have higher SINR because of the low ICI [11], [12]. In addition to this, FFR [32], [49] has a disadvantage that, I cannot use whole available spectrum, and this means that total system has lower throughput and spectral efficiency is less. In figure 3.3, we can see that; total spectrum is divided into two parts one use reuse factor 1, and one is reuse factor 3. The inner cell users only use cell center and outer cell users use cell edge zone.

3.4 SOFT FREQUENCY REUSE (SFR) METHOD

Finally, Soft Frequency Reuse (SFR) [24], [25] technique has been managed to improve both systems performance and spectral efficiency. Like FFR, SFR use two frequency band zones, cell center end cell edge. But, difference is that, SFR uses all the available spectrum in each cell when reducing the inter-cell interference [14], [52]. Cell-edge UEs can access to cell edge bandwidth while cell center UEs can access to the cell center bandwidth and can access to the cell edge bandwidth but with less priority than cell edge UEs. The restriction is on the power allocation [15], [54]. For the SFR cell center users can use two third of the total bandwidth and cell edge users can use one third of it [48]. In the cell center band, resource blocks are allocated lower transmission power because cell center user shares same bandwidth with cell edge of the neighboring cells. In contrast, cell edge users must transmit maximum power level to achieve maximum throughput rates. For this reason, cell center users have high SINR level but, cell edge users have low SINR level [14], [31]. The example of SFR scheme is shown in figure 3.4.

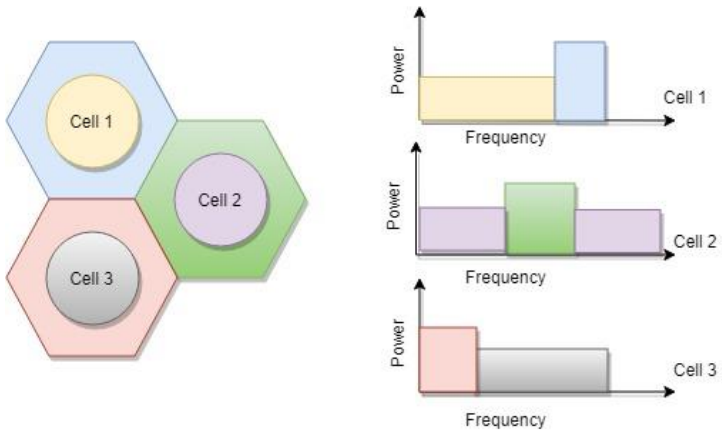

Figure 3.4: Soft Frequency Reuse (SFR) Approach.

4. SYSTEM MODEL

4.1 LTE DOWNLINK

In this thesis, I used parameters of the LTE downlink. A hexagonal cell that surrounded by six cells in a cluster for OFDMA cellular network is considered. Each cell has a base station with an omnidirectional antenna. The bandwidths are chancing as 1.4, 3, 5, 10, 15 and 20 MHz. Table 4.1 shows that how many sub-carriers and RBs are in each bandwidth for downlink and uplink.

Table 4.1: Frequency Measurement.

Bandwidth	Resource Blocks	Subcarriers (downlink)	Subcarriers (uplink)
1.4 MHz	6	73	73
3 MHz	15	181	180
5 MHz	25	301	300
10 MHz	50	601	600
15 MHz	75	901	900
20 MHz	100	1201	1200

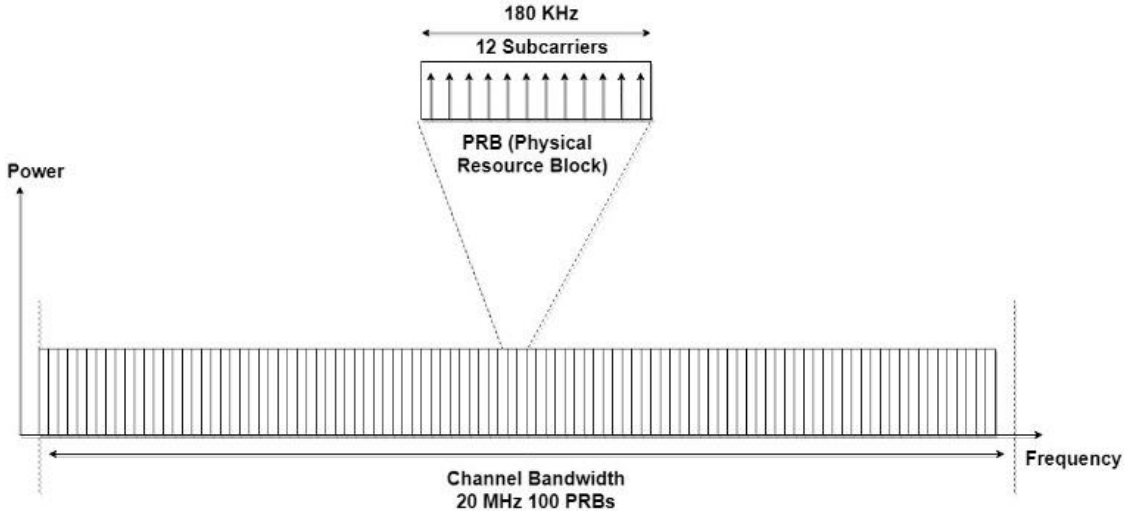

Figure 4.1: LTE Downlink OFDMA Physical Layer.

For this proposed technique, I considered 20 MHz channel bandwidth for LTE. The given bandwidth is divided into smallest bandwidth carrier that is called subcarrier. LTE subcarriers

are spaced 15 kHz apart from each other [19]. In addition to this the smallest resource for allocating to a user is Resource Block (RB). Each resource block has 12 subcarriers and 180 kHz bandwidth in the frequency domain and 1 slot (0.5 ms) in the time domain. In this system, in each time slot 100 RB are allocated and proposed algorithm determines how many RBs each user gets in a time slot.

4.2 CHANNEL MODEL

In our system, I defined a cellular system 7 base stations in one cluster. Each base station serves 10 users. Normally, in LTE systems to determine the user's throughput the adaptive coding modulation (ACM) is used on channel state information (CSI) [12]. But, in this work I decided to use Shannon's capacity formula as presented in equation 4.1 to calculate achievable user throughput on the channel;

$$T_{x,y} = B.log_2(1 + SINR_{x,y}) \tag{4.1}$$

Where $T_{x,y}$ is the throughput of user x on resource block y, B is the bandwidth of the resource block y and $SINR_{x,y}$ is the given signal to interference plus noise ratio of the user x on the y. Also, the signal to interference plus noise ratio is calculated as equation 4.2;

$$SINR_{x,y} = \frac{P_{m,s}.G_{m,s}}{N_0 + \sum_{j \in \mathrm{NC}}^{I} P_{j,n}.G_{j,n}} \tag{4.2}$$

Where $P_{m,s}$ denotes the transmitted power on RB m of serving cell and $G_{m,s}$ is the channel gain between the user m and the serving cell. Also, $P_{j,n}$ denotes the transmitted power on RB j of neighboring cell (N_C) and $G_{j,n}$ is the channel gain between the RB j and the neighboring cell. Finally, N_0 is the thermal noise density.

The overall system throughput for the serving cell can be expressed as;

$$T_{total} = \sum_{a=1}^{A} \sum_{b=1}^{B} T_{a,b} \tag{4.3}$$

Where A is the number of users is the system and B is the number of total resource blocks in the reference cell.

4.3 POWER ALLOCATION

Power allocated per RB is differ from the frequency reuse scheme [47], [55]. For the Frequency Reuse-1, each resource block has same power that is Pt = P_{total}/N where P_{total} is the total transmitting power and N is the total number of RBs in each cell. The power is uniformly distributed among the RBs. For the Reuse-3, overall spectrum is divided in 3 and the transmitted power per RB is Pt = $P_{total}/(\frac{N}{3})$ so this means that total transmitted power is 3 times greater than Reuse-1 transmitted power.

In the FFR [43,49] total RBs are allocated according to cell center and cell edge coverage. Number of RBs in the cell center is N_{center} and number of RBs in the cell edge is N_{edge}. And these number of RBs changes according to radius of center and edge cells. Total cell radius is expressed as R, cell center radius is R_{center} and cell edge radius is R_{edge}. So, I can calculate the cell center radius as R_{center} = αR where α (0<α<1) is the ratio of center radius and the cell radius. As a result, number of RBs in the cell center is calculated as N_{center} = α.N or N_{center} = N.(R_{center}/R) and number of RBs in the cell edge is calculated as N_{edge} = (N-N_{center})/3 where 3 is the reuse factor of Reuse-3 [15], [16]. For the power allocation of RBs

$$\text{Pt} = \frac{P_{total}}{N_{center}+N_{edge}} \tag{4.4}$$

In the SFR, all the spectrum is used [45]. Just like FFR, the radius and RBs are divided according to the value of α as center and edge. But, the difference is that, cell center and cell edge transmitted power levels are different from each other. If the power on the center RBs is P_{center} and on the edge P_{edge} and then this becomes βP_{edge} where β is the power ratio ($0 < \beta < 1$). If β = 1 the frequency reuse scheme becomes Reuse-1 and all the cell center and cell edge RBs have same power level.

$$P_{edge} = \frac{3P_{total}}{N(1+\beta(3-1))} \tag{4.5}$$

$$P_{center} = \beta P_{edge} \tag{4.6}$$

5. THE PROPOSED EXPERIENCE BASED DYNAMIC INTER-CELLULAR BANDWIDTH SHARING FOR LTE OFDMA NETWORKS

5.1 PACKET DELAY RATIO (PDR)

To compensate the load of the cells I proposed a dynamic algorithm that helps the adjacent cells to share resource blocks in every time slot. In every time slot I calculated packets not transmitted or received on time (packet delay) and packets transmitted and received on time. This calculation is done separately for each cell. Then I divided packets not transmitted on time by packets that are transmitted on time to calculate the system delay. This process is called Packet Delay Ratio (PDR).

$$PDR = \frac{n_{out}}{n_{tot}} \tag{5.1}$$

PDR calculation is done for every user and every cell and finally, I divided PDR by number of users belonging to cell to calculate Mean Packet Delay Ratio (MPDR).

$$MPDR = \frac{\sum_{i=1}^{i=10}}{10} \tag{5.2}$$

This parameter determines the inter-cell resource blocks allocation procedure. The cell whose MPDR values is the highest value that is called Receiver Cell (R_C). R_C can barrow resource blocks from the cell whose Lendable Bandwidth (W_L) is the highest value and I called it Donor Cell (D_C). I supposed that every cell has a lendable bandwidth and minimum bandwidth (Wmin). W_L is the bandwidth or number of resource block that donor cell can lend to the receiver cell. Also, cells have Wmin values that never lend to the other cells. Wmin is stored for cell's own users to prevent the over load and delay. There is another parameter that is called Borrowable Bandwidth (W_B). W_B is the bandwidth or number of resource blocks that R_C can borrow from the D_C. In the starting point each cell has a 100 RBs (Wi; i=1.2.3…7). Every time slot W_i, Wmin W_L and W_B are recalculated dynamically. And, cell center bandwidth (W_{in}) and cell edge bandwidth (W_{out}) are constant at initial condition and dynamically change according to resource allocation algorithm. In figure 5.1 (a), seven-cell cluster and frequency distribution are shown and in figure 6 (b), initial RBs allocation W_i, W_{in} and W_{out} are shown.

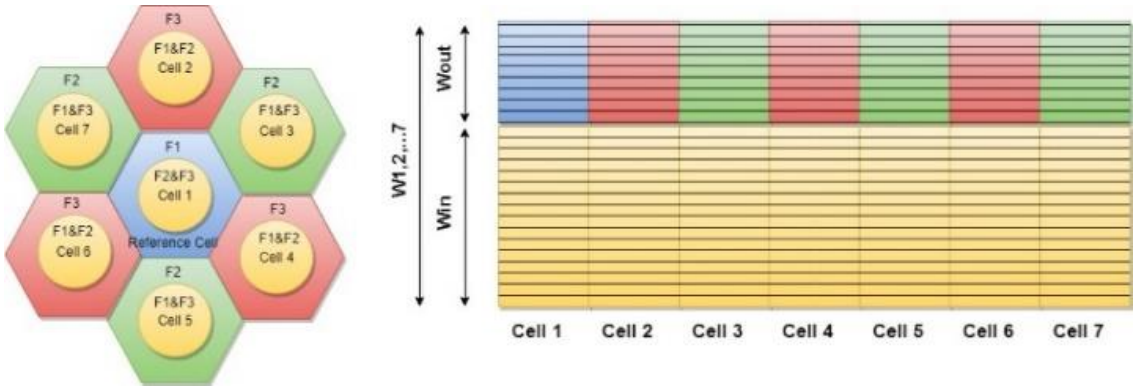

Figure 5.1: Initial System Model.

(a) Seven-Cells Hexagonal Layout (b) Initial RBs Allocation Among Cells

5.2 DYNAMIC SOFT FREQUENCY REUSE (DSFR)

In our proposed algorithm, I used SFR to allocate the RBs and I design it like a hybrid scheme. In addition to this, in our technique RBs are shared between the cells and it gives a dynamic structure to it. I called this structure Dynamic Soft Frequency Reuse (DSFR). Secondly, inner and outer cell varies by α value. When the α value changes, cell center radius increases or decreases, at the same time, cell edge area changes. According to user's demand, I can adjust the α value and this provides better fairness for the cells and users throughput. Consequently, number of cell center RBs and cell edge RBs changes with α. For instance, İf I choose α value as a 0.3, the cell center has 30 RBs and cell edge has 70 RBs. According to α value I can adjust mean cell and user's throughput and I can select best α value for the best fairness and throughput rate. In addition to this, SFR [33] uses all the RBs this means that, both users and cell throughput performance will be higher. In the proposed algorithm, due to the features of the SFR that mentioned before, allocation process occurs between the cell center of the reference cell and the cell edge of the neighboring cells.

In each time slot, DSFR determines the how many RBs allocate and reallocate between the cells. As I mentioned before W_L and W_B are calculated each time slot and allocation process takes place between R_C and D_C. At each scheduling time, some amount of RBs allocates from the donor cell to the receiver cell. If donor cell lendable bandwidth (D_CW_L) is greater than the receiver cell borrowable bandwidth (R_CW_B), donor cell can give the number of RBs that equals to R_CW_B to the receiver cell. This allocation process occurs between cell edge of the donor cell (D_CW_{out}) and cell center of the receiver cell (R_CW_{in}). So, R_CW_{in} increases as the amount of R_CW_B and D_CW_{out} decreases as the amount of R_CW_B. Else if D_CW_L is lower than the R_CW_B then

receiver cell still gets R_CW_B but, donor cell can give only amount of RBs as D_CW_L. Receiver cell can take the remaining RBs from the second highest MPDOR cell. It gives R_CW_B minus D_CW_L RBs to the receiver cell. So, R_CW_{in} increases as the amount of R_CW_B and D_CW_{out} decreases as the amount of D_CW_L. After this step new configuration is shown in figure 5.2.

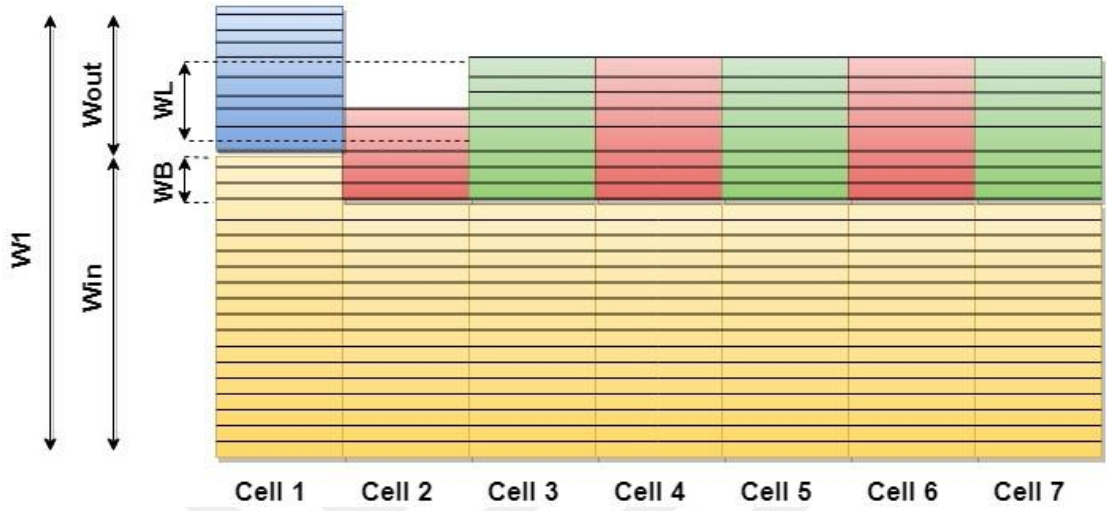

Figure 5.2: RBs allocation among cells.

In the algorithm, the EB_{DSFR} scheduling process can be seen step by step.

Algorithm: The EB_{DSFR} Scheduling Algorithm

1. **BEGIN**
2. At each scheduling time
3. **for each** cell i ∈ C **do**
4. Update (PDR(i), TRPR(i), PDOR(i), MPDOR(i))
5. Update (W_B(i), W_L(i), Wmin(i))
6. **end for**
7. Select R_C that has the highest MPDOR from all cell
8. Select D_C that has the highest W_L from the neighboring cell of R_C
9. At the starting point $W_{in}(i) = \alpha W(i)$ RBs and $W_{out}(i) = W(i) - W_{in}(i)$ RBs
10. **if** $W_L \neq 0$ **then**
11. **if** D_C $W_L(i) \geq R_CW_B$ **then**
12. $R_CW_{in}(i) \leftarrow R_CW_{in}(i) + R_CW_B$ (i)
13. $D_CW_{out}(i) \leftarrow D_CW_{out}(i) – R_CW_B$ (i)
14. **else**
15. $R_CW_{in}(i) \leftarrow R_CW_{in}(i) + R_CW_B$ (i)

16. $D_CW_{out}(i) \leftarrow D_CW_{out}(i) - D_CW_L(i)$ **then**
17. Select the second highest MPDOR from all cell except the cell that $W_L(i)$ and $W_B(i)$ **then**
18. $SD_CW_{out}(i) \leftarrow SD_CW_{out}(i) - [(R_CW_B(i) - D_CW_L(i))]$
19. **end if**
20. **end if**
21. **for** each user $u \in R_C$ **do**
22. Update (CSR(u), BER(u), R(u), EC(u) and EBPS(u)
23. **end for**
24. **if** $\alpha = 0.3$ **then**
25. # of Cell Center RBs = 30
26. # of Cell Edge RBs = 70
27. **elseif** $\alpha = 0.4$ **then**
28. # of Cell Center RBs = 40
29. # of Cell Edge RBs = 60
30. **elseif** $\alpha = 0.5$ **then**
31. # of Cell Center RBs = 50
32. # of Cell Edge RBs = 50
33. **elseif** $\alpha = 0.6$ **then**
34. # of Cell Center RBs = 60
35. # of Cell Edge RBs = 40
36. **elseif** $\alpha = 0.7$ **then**
37. # of Cell Center RBs = 7
38. # of Cell Edge RBs = 30
39. **end if**
40. **for** R_C $W_{in}(i)$
41. Allocate RBsin to all users according to EBPSin
42. First give the RBin to the user that has the highest EBPSin
43. Second give the RBin to the user that has the second highest EBPSin
44. Until all RBsin are allocate
45. **end for**
46. **for** $R_CW_{out}(i)$
47. Allocate RBsout to all users according to EBPSout

48. First give the RBout to the user that has the highest EBPSout
49. Second give the RBout to the user that has the second highest EBPSout
50. Until all RBsout are allocated
51. **end for**
52. **END**

Table 5.1: List of symbols for algorithm.

Symbol	Definition
C	Cluster
DC	Donor Cell
RC	Receiver Cell
RB	Resource Block
PDR	Packet Delay Ratio
Win(i)	Cell Center Bandwidth (RBs) of Cell i
Wout(i)	Cell Edge Bandwidth (RBs) of Cell i
WL(i)	Lendable Bandwidth (RBs) of Cell i
WB(i)	Borrowable Bandwidth (RBs) of Cell i
Wmin(i)	Minimum Bandwidth (RBs) of Cell i
W(i)	Total Number of Resource Blocks of the Cell i
SFR	Soft Frequency Reuse
FFR	Fractional Frequency Reuse
EBPS	Experiment Based Packet Scheduler
EB_DSFR	Experiment Based Dynamic Soft Frequency Reuse

5.3 EXPERINCE BASED-PACKET SCHEDULER

Another decision occurs about which user will receive the RB first. For this decision, I used our recent proposed technique that is called Experience-Based Packet Scheduler (EBPS) [13], [34].

EBPS determines the placements of the users that they get the RBs. In addition to this, it provides fairness among users. The experience-based packet scheduler is formulized under the experience classifier $EC_u(n)$ and it is calculated by using user's previous call success rate $CSR_u(n)$ the previous average throughput rate $Rp_u(n)$ and bit error rate $BER_u(n)$. Furthermore, quality of service $QoS_u(n)$ instant throughput $Ri_u(n)$that has two coefficients (Ɵ and ɸ) and channel load (L) are considered in this calculation and all these parameters are divided by average throughput $Ra_u(n)$. At the end of this process I got a decision metric and user who experience poor service quality previously will be the priority of these packets. The main formula can be seen in formula 5.3 that belonging EBPS.

$$EBPS_u(n) = \frac{QoS_u(n)\Theta Ri_u(n)^{\phi}(n)EC_u(n)L}{Ra_u(n)} \tag{5.3}$$

Users are divided into various classes according to the amount of data they want and what they pay based on different classes. The system provides more throughput per unit time to high class users. Thus, the quality of service provided to users increases. Users can be further subdivided into traffic classes. The data transmission command center can define user's priority and assign more throughput to them.

Users' previous time experiences are analyzed and where the time interval can be hours, minutes or seconds as determined by the operator. Throughput is taken as an average over a specific time interval for each user. The experience classifier dynamically calculates quality of service for the users in the network.

Consequently, the EBPS's aim is to eliminate the unfair treatment by ensuring that the rights of high subscription class users and to maximize data transmission for the entire system.

5.3.1 Experience Classifier

Experience Classifier $EC_u(n)$ assesses the previous service received by users from the base station. The priority for fairness is to generate a metric considering user's previous call success rate $CSR_u(n)$ the previous average throughput rate $Rp_u(n)$ and bit error rate $BER_u(n)$ and the users who have previously experienced poor service in these three parameters.

$$EC_u(n) = \frac{\mathrm{BERu(n)}}{Rp_u(n) * \mathrm{CSRu(n)}} \tag{5.4}$$

Formula 5.4 shows the equation of $EC_u(n)$. After calculating the $EC_u(n)$ values results are converted to integers as 1,2,3,4 and 5. The users with a small number is given a higher $EC_u(n)$ values. Therefore, the user had previously miserable experience take precedence.

When $EC_u(n)$ is less than 10^{-6} the value is considered 5, when the $EC_u(n)$ is between 10^{-6} and 10^{-4} the value is considered 4, when $EC_u(n)$ is between 10^{-4} and 10^{-2} the value is considered 3, when $EC_u(n)$ is between 10^{-2} and 1 the value is considered 2 and when $EC_u(n)$ is between 1 and 100 it is considered 1.

5.3.1.1 Call success rate

Call success rate is a proportion of total call attempts to successful calls. Thus, all the users in the receiver cell are ranked according to the EBPS values and RB allocation starts. Call setup procedure happens if the result of call attempt is successful. In some cases, because of technical reasons, call setup can be failed. These call trials are referred as failure attempts. When the call cannot establish because of the busy link, the call process is not defined as failed call. Call also may be stopped due to the undesirable reasons after it has been set up. The case is called as call drop. At wire connection, the call success rate reaches 99.9% but, in the wireless one it stays between 90% and 98%. The success and failure call in the simulation are simulated and calculated as a random and formula 5.5 defines it.

$$CSR_u(n) = CSSR_u(n)*(1- CDR_u(n)) \quad (5.5)$$

In this formula, $CSSR_u(n)$ is Call Setup Success Rate and $CDR_u(n)$ is Call Drop Rate.

5.3.1.2 Throughput

Throughput $Ra_u(n)$ is the users' mean data rate at any time. Based on the instantaneous condition of the channel, user request data from the base station, and data send to the users according to channel load condition. In this mean throughput we determined the time interval of the user $Ti_u(n)$ as a hours, minutes or seconds as determined by the operator. Time interval is the time that we take how many times before. Also, instant throughput $Ri_u(n)$ can send as a resource block in each TTI and has two coefficients (Θ and ϕ). Every TTI we add instant throughput $Ri_u(n)$ to the previous average throughput rate $Rp_u(n)$ and we calculate users' average data rate $Ra_u(n)$.

5.3.1.3 Bit error rate

Bit Error Rate $BER_u(n)$ is the percentage of the inaccurate bits. We can find it by dividing the number of incorrect bits by total bits. The noise, interference, deviation of signal and synchronization errors may cause these errors to occur. $BER_u(n)$ is calculated as follows.

$$BER_u(n) = \frac{\text{Number of faulty bits}}{\text{Number of total transferred bits}} \quad (5.6)$$

5.3.2 Quality of Service

The system aims to allocate more throughputs to the high-class users and this packet scheduler makes it possible. Users are divided into various classes according to the amount of data they want, and for this purpose, they pay different bills. $QoS_u(n)$ is designed to avoid unfairness and users takes the right their moneys that they pay.

Which class belongs to user is determined by the traffic class and data transmission command center and at the same time which user has more priority, the center decides to transmit more throughputs to it. $QoS_u(n)$ has three different classes that are platinum, gold and silver. These classes are represented as integers as follows;

Platinum =16,

Gold=4,

Silver=1

5.3.3 Channel Load

Base station load conditions are variable by population density. Each base station is specifically capable of providing service. More cells are needed to respond to increasing traffic and this means that extra cost for the mobile operators. If the operators do not increase the base stations, this cause negative interactions. These interactions can cause noise and interference that effect the signal quality bad way. In my thesis, each cell has 10 users and channel load is always same. But, in a different scenario channel load is important factor to determine the users' priority.

Traffic engineers serve the same number of users in the smaller area, reducing the base station coverage and eliminating capacity issues [51]. Therefore, the number of base stations becomes higher to overcome this problem and they serve smaller area. Each base station has 120 degree channels and they can serve more users.

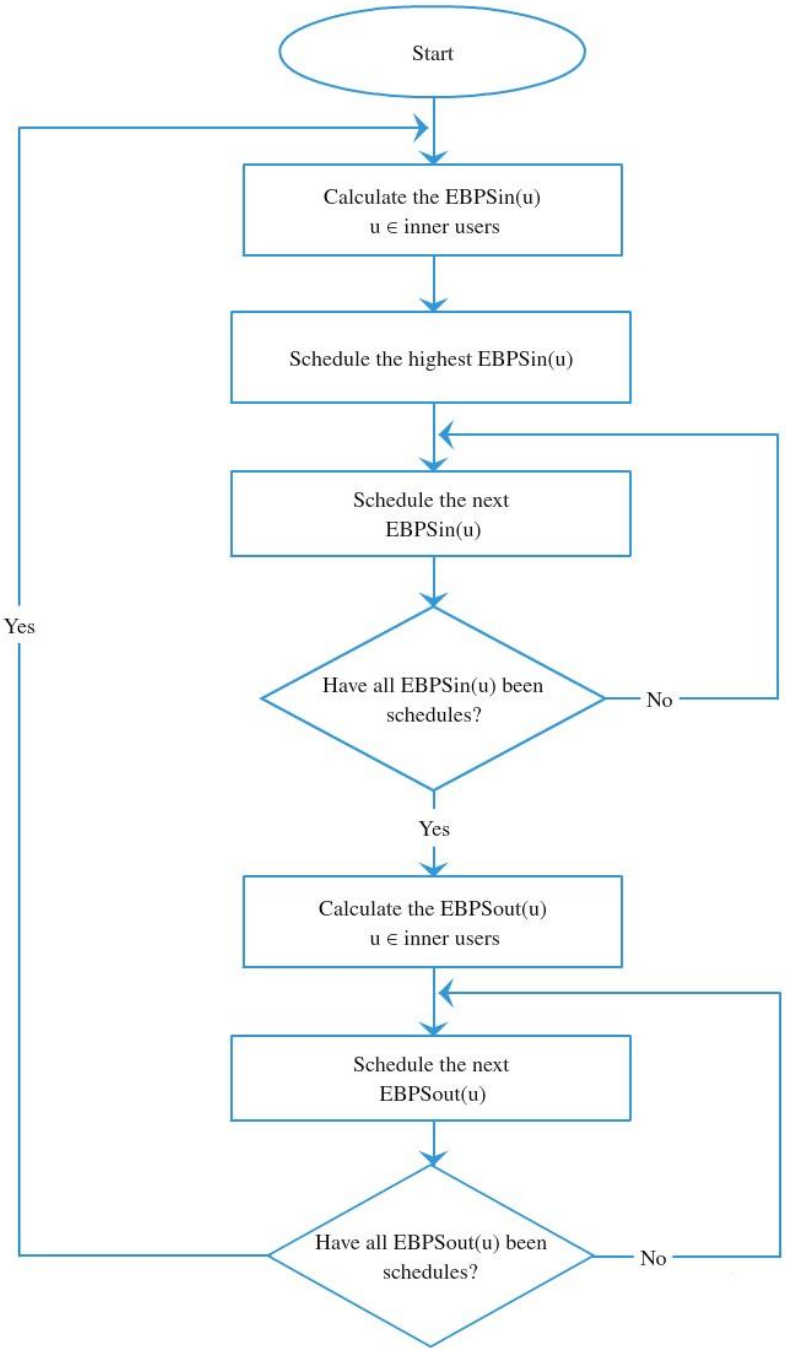

Figure 5.3: Flow chart for EBPS.

5.4 SIGNAL TO INTERFERENCE PLUS NOISE RATIO (SINR) METHOD

Another issue is to find out where users are in the cell. In other words, I need to determine which users belongs to cell center and which ones belongs to cell edge. There are two different methods to determine the inner and outer cell user. One is distance method and the other one is SINR method. In the distance method, if the user has a smaller distance from the threshold values it means that the user is in the inner region and if the user has a greater distance from the threshold values it means that the user is in the outer region. In the SINR method, if the user has a greater

SINR value from the threshold value it means that the user is in the inner region and if the user has a smaller SINR value from the threshold value it means that the user is in the outer region. The distance and SINR threshold values are determined before the process. I use SINR method in our technique. I determine the inner and outer region SINR threshold values and then I placed the users in a random way in the inner and outer cells. After the determination of the users SINR values according to formula 4.2, I used maximum SINR method (MaxSINR) to allocate the RBs to the users. Each user has a different SINR value according to its position of the cell. This means that, each user has a different SINR value for each RB. So, first I selected the user who has maximum EBPS value for the cell edge and cell center separately and then I selected the RB that is the highest SINR value for that user. In other words, I allocated the RB y to the user x that has the highest m_{xy} in a time slot. This process continues until all the RBs are allocated to all users in a time slot. As a numerical example, suppose the α value is 0.3 and there are 5 users in the cell center of the reference cell. So, there are 30 RBs in the inner cell and every user can get 6 RBs in one-time slot. This allocation process is performed as a loop that starts max SINR of the highest EBPS value user. And proceeds from high to low ones.

6. SIMULATION RESULTS AND ANALYSIS

6.1 COMPARISON WITH OTHER ICIC TECHNIQUES IN THE LITERATURE

In this scenario, I compared our proposed algorithm (EB_{DSFR}) with the other ICIC techniques in the literature. The average throughput, cell-edge throughput and cell-center throughput of the reference cell and user's fairness [29] are considered as major referencing elements for performance evaluation. I took account of the frequency reuse one, frequency reuse three, FFR and SFR as the reference scheme for performance comparison with the proposed technique EB_{DSFR}. In table 6.1, simulation parameters are shown.

Table 6.1: Simulation Parameters.

Parameter	**Value**
Cell geometry	Hexagonal
Cell radius	1 km
Cell center radius	Variable according to α
Operating bandwidth	20 MHz
Number of users per cell	10
Subcarriers frequency	15 KHz (1 RB 12 Subcarriers)
RB bandwidth	180 KHz
Number of RBs	100
TTI	1 ms
Thermal noise density	-174 dBm/Hz
BS transmit power	20 W (43 dBm)
Scheduler	Experiment Based Packet Scheduler
SFR power ratio (β)	0.25
Pathloss model	15.3 + 127.6 log10(D)

Instead of focusing on the performance of the overall system, I focused on performance of a specific cell, which is called reference cell. In our proposed algorithm I considered Cell 1 as a reference cell. Performance of the reference cell is determined by the its own eNodeB and other adjacent eNodeBs. In this work, the reference cell is the center cell and it is surrounded by six adjacent cells shown in figure 5.1 (a).

In this thesis, an LTE based OFDMA cellular system is used to simulate proposed and reference schemes. I used 19 cells system layout and I just focused 7 cells cluster at the center of the whole system. There are 10 users in each cell and they randomly distributed inside the cells. Also, each cell has own base station at the center of them and use omnidirectional antenna. The cells geometry is assumed as hexagonal and their radius are 1 km. The operating bandwidth is 20 MHz and 100 RBs are used for the allocation process in each cell. RBs have a bandwidth of 180 KHz and all RBs have 12 subcarriers having a bandwidth of 15 KHz.

In our simulation results, fairness index is so important to determine if the users share system resources in a fair way. There are many different types of fairness calculation methods and I used Raj Jain's fairness equation [18];

$$J(X_1, X_2, \dots X_n) = \frac{(\sum_{i=1}^{N} X_i)^2}{N.\sum_{i=1}^{N} {X_i}^2} \quad (6.1)$$

Where J is the fairness of a set of throughput values of the users, N is the number of users in the system and X_i is the average throughput value of the user i. The result ranges from $\frac{1}{N}$ (worst case) to 1 (best case) and fairness index becomes maximum when all the users have same throughput rates.

6.1.1 Comparison According to Throughput

In the Table 6.2, numerical values of the comparisons are shown. All the techniques simulated for the different α values. Detailed explanations are in the follwing charts.

Table 6.2: Simulation Results for Reuse-1, Reuse-3, FFR, SFR and EB_{DSFR} with different α values.

Average User Throughput (Mbps)					
	α=0.3	α=0.4	α=0.5	α=0.6	α=0.7
Reuse-1	6.30	6.30	6.30	6.30	6.30

Reuse-3	2.89	2.89	2.89	2.89	2.89
FFR	4.22	4.8	5.32	5.85	6.38
SFR	6.15	6.41	6.66	6.85	7.09
EB_{DSFR}	6.76	7.02	7.24	7.50	7.68
Average Cell Center User Throughput (Mbps)					
	α=0.3	α=0.4	α=0.5	α=0.6	α=0.7
Reuse-1	7.67	7.67	7.67	7.67	7.67
Reuse-3	3.06	3.06	3.06	3.06	3.06
FFR	4.95	6.58	8.09	9.77	11.34
SFR	4.68	6.11	7.68	9.11	10.67
EB_{DSFR}	5.98	7.33	8.85	10.4	11.9
Average Cell Edge User Throughput (Mbps)					
	α=0.3	α=0.4	α=0.5	α=0.6	α=0.7
Reuse-1	4.93	4.93	4.93	4.93	4.93
Reuse-3	2.71	2.71	2.71	2.71	2.71
FFR	3.48	3.02	2.55	1.93	1.42
SFR	7.63	6.71	5.63	4.59	3.51
EB_{DSFR}	7.63	6.71	5.63	4.59	3.51
Fairness Percentage (%)					
	α=0.3	α=0.4	α=0.5	α=0.6	α=0.7
Reuse-1	95	95	95	95	95
Reuse-3	99	99	99	99	99
FFR	98	98	96	88	79

SFR	98	99	98	90	80
EB_{DSFR}	97	98	95	87	77

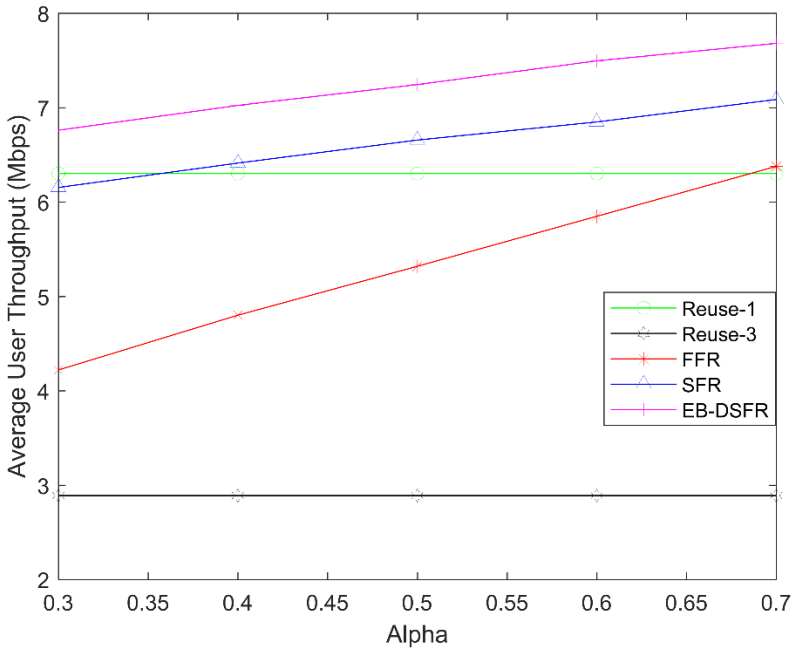

Figure 6.1: Average user throughput for Reuse-1, Reuse-3, FFR, SFR and EB_{DSFR} with different α values.

First, in figure 6.1, we can see the average user throughput values for different frequency reuse techniques and I compared these techniques with our proposed EB_{DSFR} technique. I used Round Robin (RR) scheduling algorithm for these four reuse techniques. Also, for this comparison, I selected different α values (0.3, 0.4, 0.5, 0.6 and 0.7) that is ratio of the cell center radius to cell radius. Also, I just focused on the reference cell (cell 1) and I supposed that, reference cell has the highest MPDOR (receiver cell) and other 6 cells can be donor cell according to their $W_L(i)$ values.

For Reuse-3, users have a less average throughput because of the less RBs. Just 1/3 of the available spectrum can be used and there are approximately 33 RBs in the cell so, users in the cell have less resources to allocate. In the Reuse-1 technique, all the spectrum is used and there are 100 RBs in the cell. Average user throughput is higher comparing to Reuse-3 but, adjacent cells use same frequency, and this causes lower SINR for the users. This means that overall system capacity is affected, and average throughput decreases comparing to SFR and EB_{DSFR}. In addition to this, in the Reuse-1 and reuse-3 there is no need to use α and average user

throughput is constant each α values. When we look at the FFR technique, average throughput values increase when the α values increase. In the FFR, cell center uses Reuse-1 method and cell center uses Reuse-3 method. This provides better SINR values for the users but, in the cell edge zone 1/3 of the available spectrum can be used. This creates less RBs for users. When I compare FFR with the SFR and EB_{DSFR}, users have less average throughput values. Also, we can see from figure 6.1, when the α increases, average throughput increases directly proportional because of the increasing available bandwidth. We can clearly see that, SFR and EB_{DSFR} techniques are most efficient techniques in terms of the user average throughput. Because in the SFR method, all the available spectrum can be used.

In addition to this, less inter-cell interference increases SINR for the users and user average throughput increases. Especially, cell center users have better SINR so, when α increases, throughput values increase. The difference between SFR and EB_{DSFR} is resource allocation. We can see in figure 6.1, in the EB_{DSFR} method, average user throughput is higher than the SFR method approximately 10%. Because, reference cell can receive RBs in the neighboring cells and this means that more RBs can be used for the users in our proposed method. And when the α increases, throughput values increase for the users as in SFR.

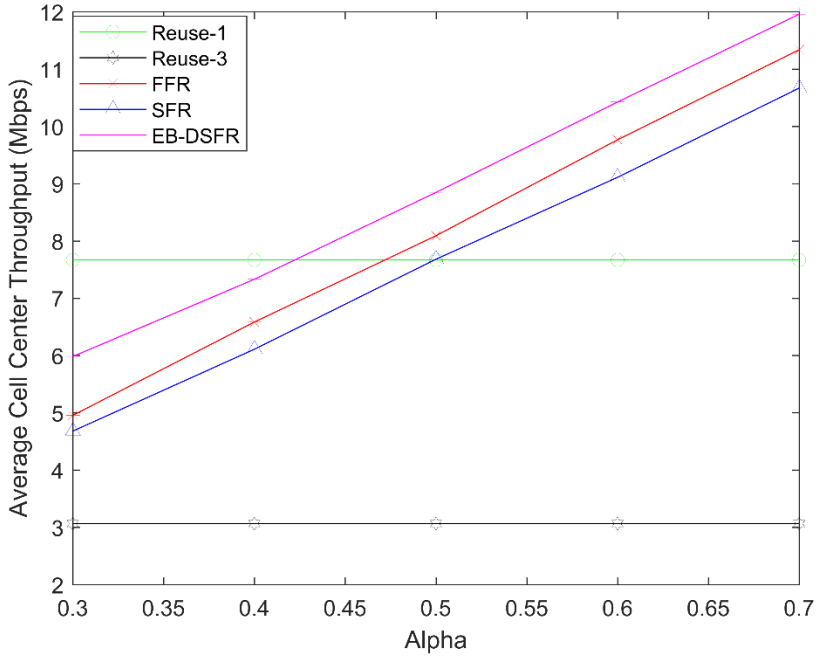

Figure 6.2: Average cell center user throughput for Reuse-1, Reuse-3, FFR, SFR and EB_{DSFR} with different α values.

As we see in figure 6.2, for FFR, SFR and EB_{DSFR} when α increases average cell center user throughput increases because number of cell center RBs increases. This means that, more

resources can be allocated to user and they can access more RBs in one slot time. The difference is that, FFR has better performance than SFR. Because in the SFR method, cell center user shares same bandwidth with cell edge of the neighboring cells. However, in FFR method, cell center user does not share same bandwidth with cell edge of the neighboring cells. They share same bandwidth with cell center of the neighboring cells. The distance between them is more and they have better SINR values. So, average cell center user throughput is better for the FFR. As I mentioned before, in Reuse-1 and Reuse-3 average cell center user throughput is constant. When α equals to 0.3 and 0.4 Reuse-1 has better performance comparing to other methods. After α becomes 0.5, RBs increases sufficiently and their performance becomes better. On the other hands, EB_{DSFR} has better performance because, it receives RBs from the neighboring cells to the center of it. And Reuse-3 method has worst performance.

In figure 6.3, we can obviously see that. when α increases average cell edge user throughput decreases for FFR, SFR and EB_{DSFR} because number of cell edge RBs decreases. EB_{DSFR} and SFR have almost same throughput values. In our proposed method, cell edge of the reference cell does not receive any RBs from its neighbors. Also, for the cell edge users FFR has bad performance because of the available bandwidth. Reuse-1 method has best performance for the 0.6 and 0.7 α values.

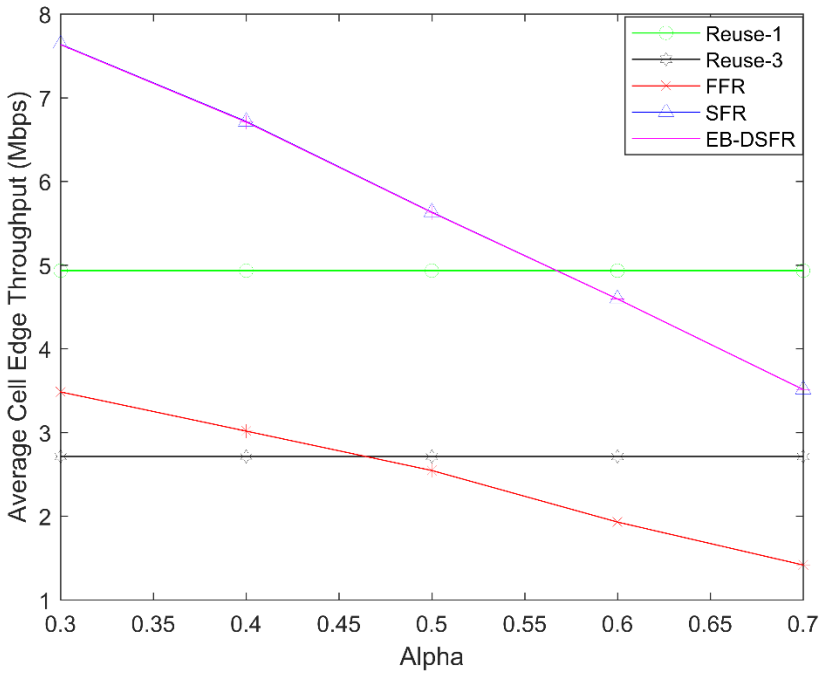

Figure 6.3: Average cell edge user throughput for Reuse-1, Reuse-3, FFR, SFR and EB_{DSFR} with different α values.

As we see in figure 6.4, Reuse-3 technique has the highest throughput fairness index among all the frequency reuse techniques.

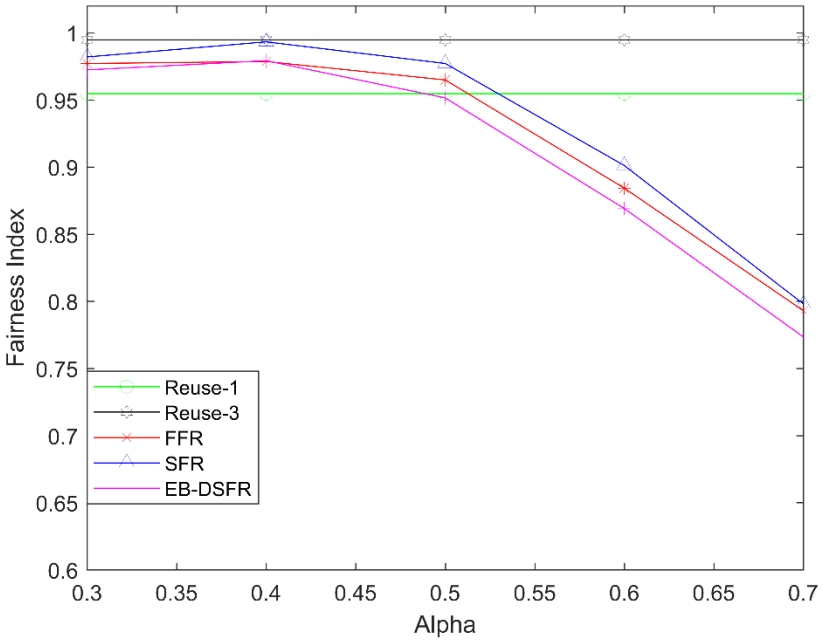

Figure 6.4: Fairness index for Reuse-1, Reuse-3, FFR, SFR and EBDSFR with different α values.

In Reuse-3, because of inter-cell interference is removed, all the users have almost same throughput rates, and this increases the fairness index. When I compare Reuse-1 method with Reuse-3 method, Reuse-1 method has more ICI, and this leads worse fairness for it. On the other hands, SFR, FFR and EB_{DSFR} have best fairness index performance at 0.4 α value. When α is 0.4, cell edge has more RBs than the cell center but, cell center users have better SINR. So, average cell center and cell edge user's throughput are balanced for this reason. With the increase of the α value, RBs are increase for the cell center, and fairness index decreases. In the simulation I use Round Robin (RR) scheduling algorithm for the other techniques and we can see that RR is fairer than our proposed technique that used EBPS as a scheduler algorithm. Generally, SFR is fairer than the FFR and my proposed algorithm EB_{DSFR}. Normally, SFR and EB_{DSFR} can be same fairness index but, in my proposed method I used different scheduler technique and because of this reason SFR is fairer than the EB_{DSFR}. For other methods, I used RR scheduler technique and we know that in the RR method RBs are assigned to each user in equal portion and in circular order without priority.

6.1.2 Comparison According to Delay

Also, I measured the average user packets delay with using CPU bursts method. In our simulation I used MATLAB to simulate the algorithms and I used computer that has Intel(R) Core (TM) i5-3230M CPU @ 2.60 GHz processor. For the all techniques, RBs are allocated among the users every TTI and I measured the execution time of allocation process. The RBs enter the queue and allocate the users by turns.

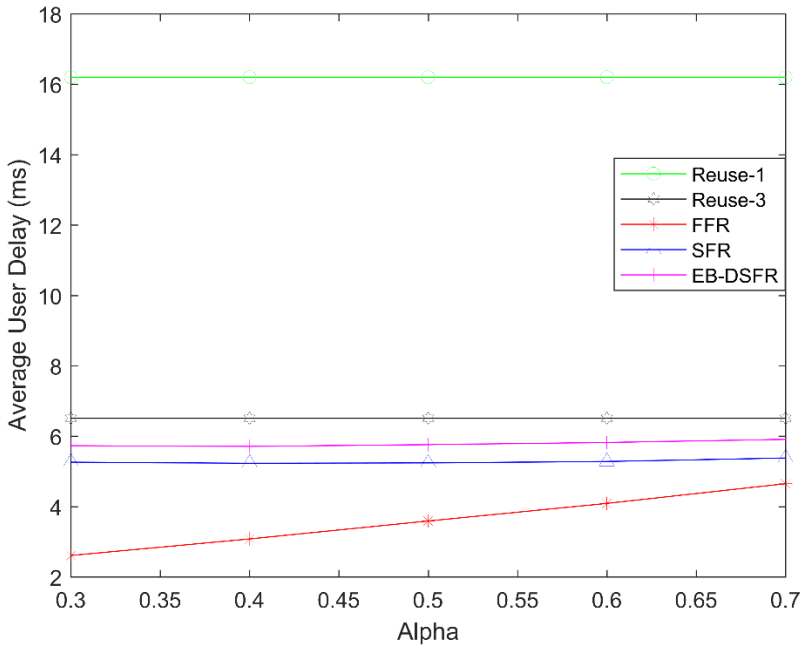

Figure 6.5: Average user delay for Reuse-1, Reuse-3, FFR, SFR and EB_{DSFR} with different α values.

In figure 6.5, we can see that, mean users delay for Reuse-1, Reuse-3, FFR, SFR and EB_{DSFR} for different α values. In each technique, there are 10 users in the simulation medium and 5 of them are in the cell center and 5 of them are in the cell edge. As we see in the figure, Reuse-1 and Reuse-3 have constant RBs that are in the queue and they don't depend on the α values. For this reason, the delays are constant for them. Also, EB_{DSFR} and SFR and FFR have constant RBs for every α values in the queue and delays are almost constant. When the α increases the delay of FFR increases directly proportional because of the increasing number of RBs in the queue. EB_{DSFR} has more delay than the FFR and SFR because it has more RBs in the queue. Although, EB_{DSFR} has more delay than the FFR and SFR, it provides better throughput values.

In figure 6.6, we can see that, mean cell center users delay for Reuse-1, Reuse-3, FFR, SFR and EB_{DSFR} for different α values. As we see in the figure again, Reuse-1 and Reuse-3 have constant RBs that are in the queue and the delays are constant. When the α increases the delays of EB_{DSFR}

SFR and FFR increase. The reason of this situation, when α values increases, the number of RBs increase in the cell center. Furthermore, EB_{DSFR} has more RBs in the center cell because of the borrowed RBs and it has more delay compared to the SFR and FFR. The delays of SFR and FFR techniques are approximately same for all α values as seen in the figure. After α=0.55 EB_{DSFR}, SFR and FFR have more delays than the Reuse3 technique.

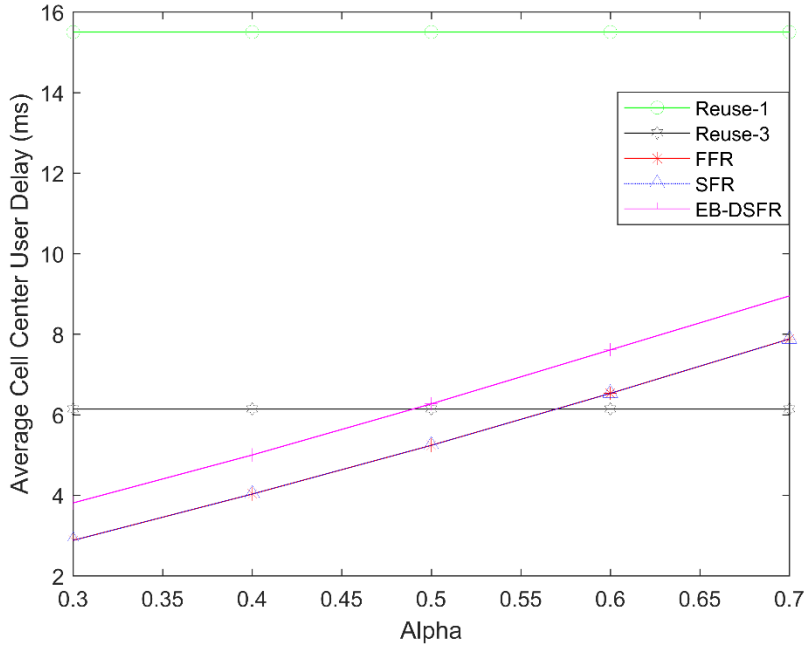

Figure 6.6: Average cell center user delay for Reuse-1, Reuse-3, FFR, SFR and EB_{DSFR} with different α values.

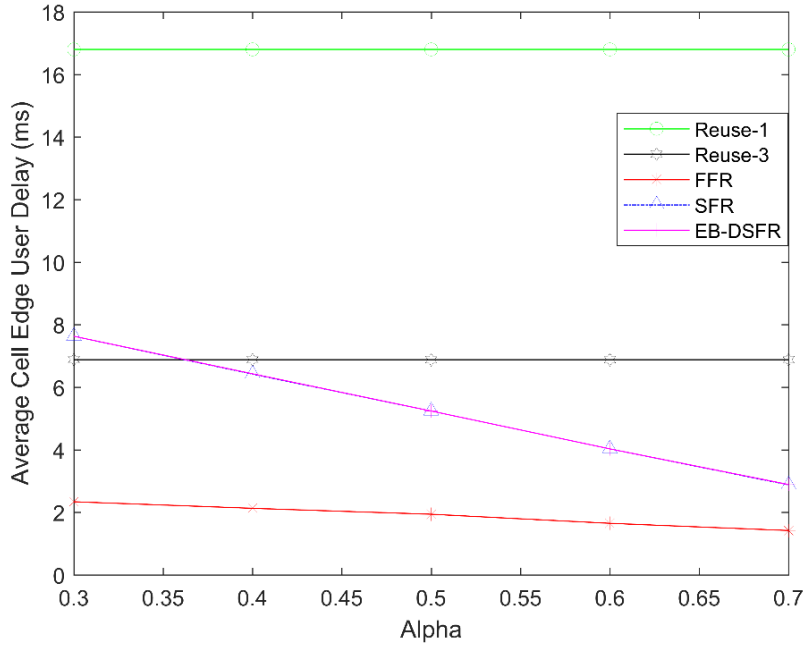

Figure 6.7: Average cell edge user delay for Reuse-1, Reuse-3, FFR, SFR and EB_{DSFR} with different α values.

As we see in figure 6.7, when the α increases the delays of EB_{DSFR}, SFR and FFR decrease because of the decreasing number of RBs. FFR techniques are less delays from the EB_{DSFR} and SFR. It uses 1/3 of the RBs in the cell edge and there are less RBs in the queue. This means that, less process time needed to execute. In addition to this, RBs of the Reuse-3 and Reuse-1 are constant again and delays are also constants.

6.1.3 Comparison According to PDR Percentage

As I mentioned above, in each TTI, I calculated packets not transmitted or received on time and packets transmitted and received on time. Then I divided packets not transmitted on time into whole packets to calculate the system delay as shown in formula 7. I called this process Packet Delay Ratio (PDR). PDR calculation is done for every user in the reference cell. I set the delay threshold of each RBs 10 ms and PDR target is 25%. If the PDR target is a user more than 25% then I supposed that this user is dissatisfied.

In figure 6.8, we can see that, mean user PDR percentages for Reuse-1, Reuse-3, FFR, SFR and EB_{DSFR} for different α values. When we compared the PDOR percentage of the EB_{DSFR} with the SFR, they have nearly same characteristics but, the PDOR percentage of the EB_{DSFR} is higher.

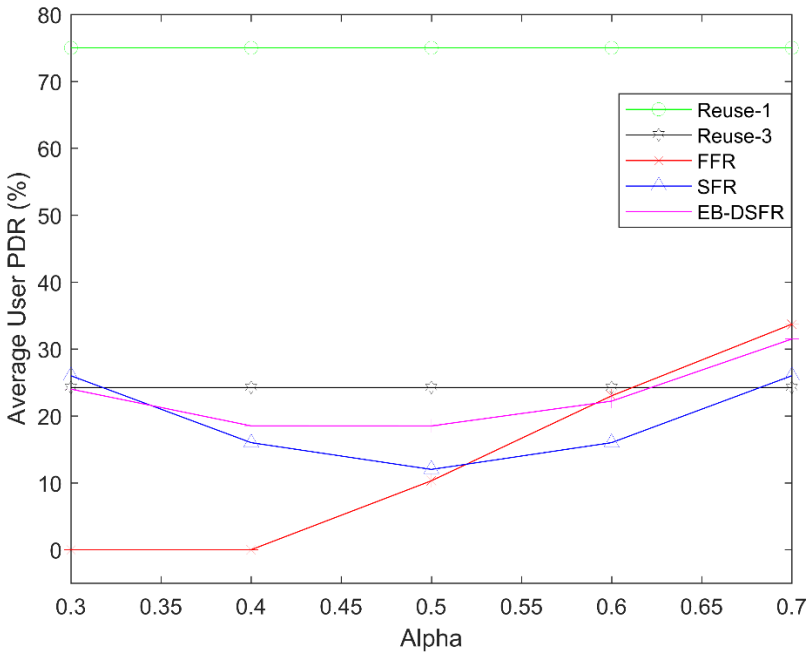

Figure 6.8: Average user PDR (%) for Reuse-1, Reuse-3, FFR, SFR and EB_{DSFR} with different α values.

This is caused by the number of total RBs of the EB_{DSFR} is more than the number of total RBs of the SFR. Because EB_{DSFR} borrows RBs from its neighbors and it has more RBs in one TTI.

So, the RBs in the queue is more. When the α increases the PDR (%) of FFR increases directly proportional because of the increasing number of RBs in the queue. It changes from 0% to 33.7%. Also, EB_{DSFR} has more PDR % up to α=0.6 compared to the FFR. After this value PDR % of the EB_{DSFR} becomes smaller than the FFR. This is caused by the number of total RBs of the EB_{DSFR} is more than the number of total RBs of the FFR. So, average PDR values of EB_{DSFR} can be higher than the FFR. In addition, Reuse-3 and Reuse-1 have constant RBs that are in the queue. For this reason, PDR percentages are almost constant. Although, EB_{DSFR} has more PDR % for some cases than the FFR and SFR, it provides better throughput values because of the number of RBs.

As we see in figure 6.9, when the α increases the PDR % of EB_{DSFR}, SFR and FFR increase. The reason of this, when α values increases, the number of RBs increase in the cell center and delays are also increasing. The PDR percentages of EB_{DSFR}, SFR and FFR techniques are approximately same for all α values as seen in the figure. Because, they have approximately same delays for all α. For Reuse-3 and Reuse-1 techniques, RBs are constant again and delays and PDR percentages also constant.

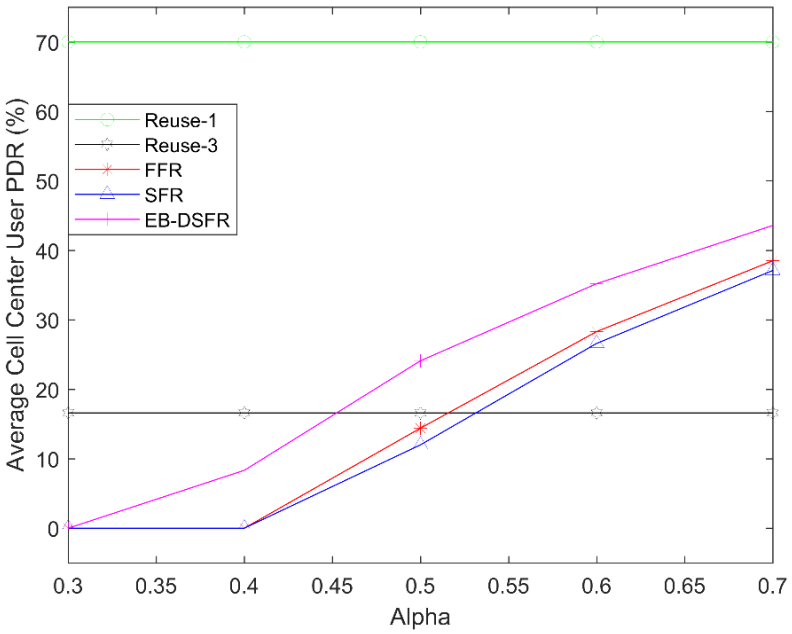

Figure 6.9: Average cell center user PDR (%) for Reuse-1, Reuse-3, FFR, SFR and EB_{DSFR} with different α values.

We can see in figure 6.10, when the α increases the PDR % of EB_{DSFR} and SFR decreases because of the decreasing number of RBs and delays. At the same time, FFR techniques has no RBs in delay outage. It uses 1/3 of the RBs in the cell edge and there are less RBs in the queue.

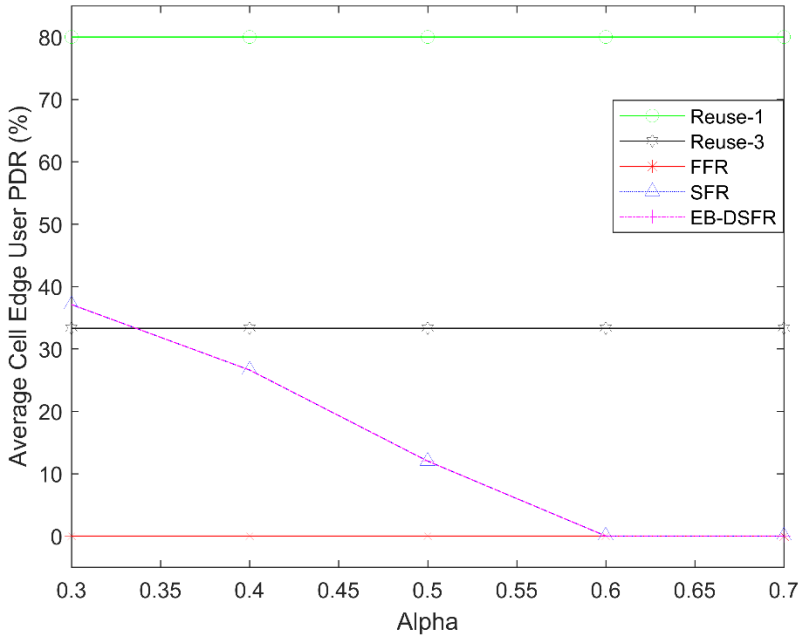

Figure 6.10: Average cell edge user PDR (%) for Reuse-1, Reuse-3, FFR, SFR and EB_{DSFR} with different α values.

After α reaches 0.6 value EB_{DSFR} has no delay because of the decreasing number of RBs. Finally, for Reuse-1, PDR percentage is constant as 80% and for Reuse-3, PDR percentage is constant as 33.3%.

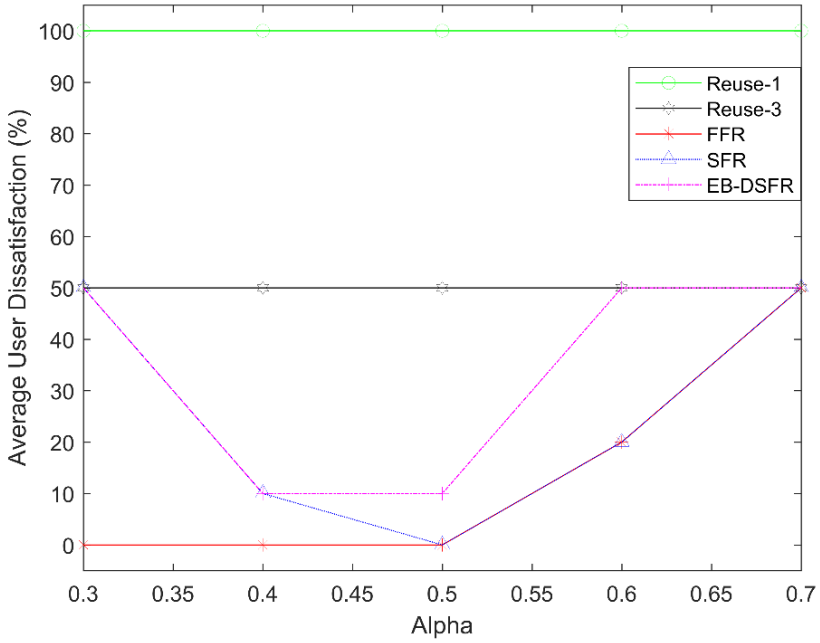

Figure 6.11: Average user dissatisfaction (%) for Reuse-1, Reuse-3, FFR, SFR and EB_{DSFR} with different α values.

In figure 6.11, we can see that, average user dissatisfaction percentages for Reuse-1, Reuse-3, FFR, SFR and EB_{DSFR} for different α values. EB_{DSFR} and SFR have same dissatisfaction percentages, becaues they have same average user delays. FFR has best dissatisfaction ratio up to α=0.5 and after that value, EB_{DSFR} has same dissatisfaction ratio with the FFR. Reuse-1 and Reuse-3 have constant dissatisfaction ratios. For Reuse-1, dissatisfaction percentage is constant as 100% and for Reuse-3, it is constant as 50%. Users are more satisfied in the FFR technique as a delay performance but, as a throughput performance they are more dissatisfied in the EB_{DSFR} technique.

6.1.4 Comparison According to SINR

In this scenario, I compared our proposed algorithm EB_{DSFR} with the other ICI techniques in the literature. I took user's SINR values as a major referencing element for this comparison. As I did before, I focused on performance of a reference cell that is cell 1. Cell 1 is the center cell and other 6 cells surround it.

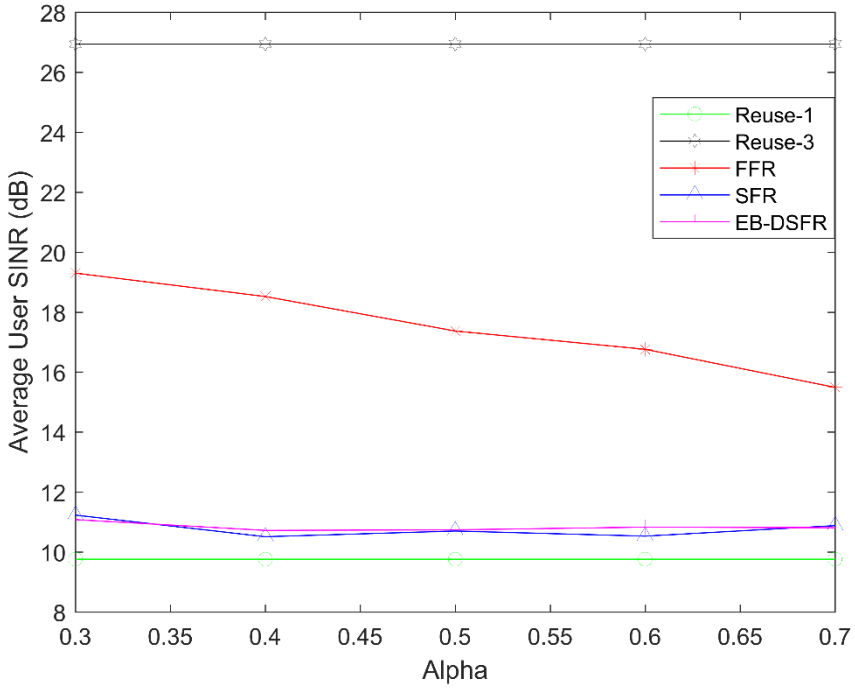

Figure 6.12: Average user SINR for Reuse-1, Reuse-3, FFR, SFR and EB_{DSFR} with different α values.

In figure 6.12, we can see the average user SINR values of my proposed EB_{DSFR} other ICI techniques in the literature that are Reuse-1, Reuse-3, SFR and FFR. As I mentioned above; In Reuse-3 method, all the adjacent cells use different frequency, and all the users have very high SINR values. As opposed to this, In Reuse-1 method, all the adjacent cells use same frequency,

and all the users have very low SINR values. In the FFR method, cell center zone uses frequency reuse-1 method and cell edge zone uses frequency reuse-3 method. Also, cell center and cell edge use different frequency band, and this provides better SINR values compared to SFR and EB_{DSFR}. When we look at the SINR values of the SFR and EB_{DSFR}, in the cell center band, frequency spectrum is allocated lower transmission power because cell center user shares same bandwidth with cell edge of the neighboring cells cell center users have good SINR values but, cell edge users have low SINR values. SFR and EB_{DSFR} have less SINR values compared to the other techniques, but they use all the available spectrum and have better throughput values.

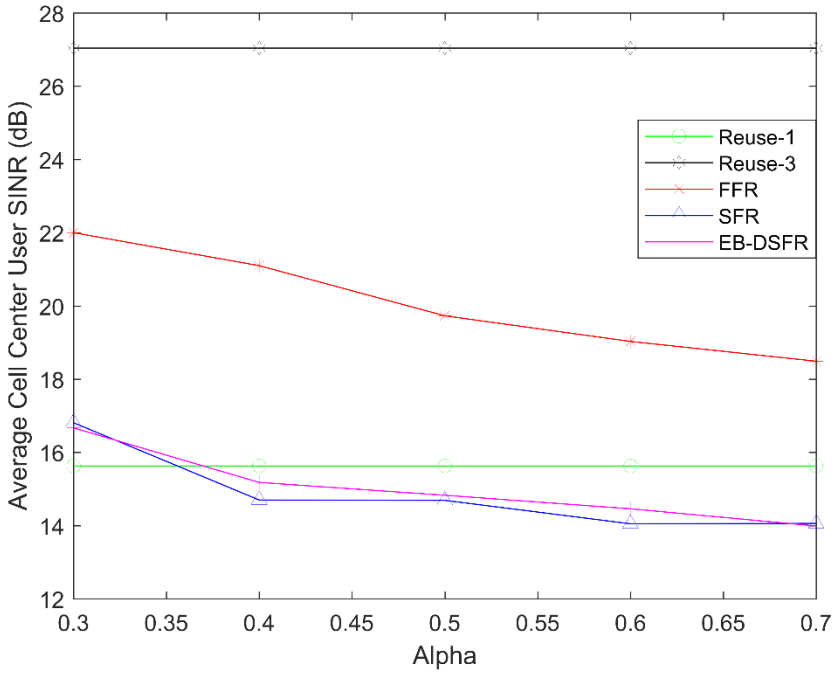

Figure 6.13: Average cell center user SINR for Reuse-1, Reuse-3, FFR, SFR and EB_{DSFR} with different α values.

As we seen in the figure 6.13, Reuse-3 method has the highest cell center SINR values. As I explained before, all neighboring cell use different frequency, and this causes high SINR values but, lower throughput values. In Reuse-1 method, all the adjacent cells use same frequency, and users in the center cell have lower SINR values compared to the Reuse-3. Our proposed method EB_{DSFR} and SFR method have worst SINR values as we see. In the EB_{DSFR} and SFR methods, cell center users use same bandwidth with the neighboring cells' cell edges, but in FFR method it is not like this. They use same bandwidth with neighboring cells' cell center. Because of the more distance, they have better SINR values than the EB_{DSFR} and SFR methods. In addition to this, when α increases, the SINR values of the EB_{DSFR}, SFR and FFR decreases. Because, cell

center expands and users who locates in the cell center are away from the base station. This causes less average SINR values.

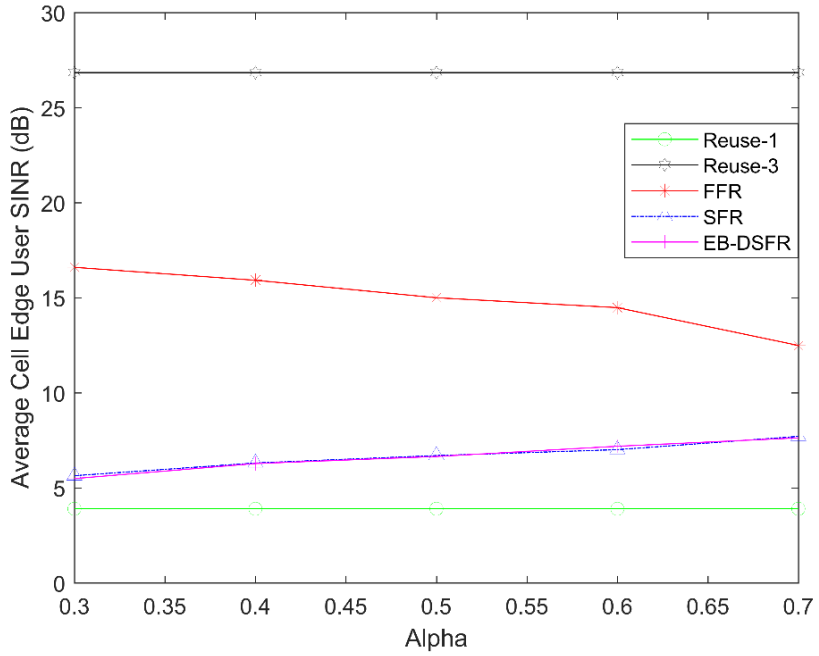

Figure 6.14: Average cell edge user SINR for Reuse-1, Reuse-3, FFR, SFR and EB_{DSFR} with different α values.

In figure 6.14, we can see that, Reuse-3 method has the highest cell center SINR values again. In Reuse-1 method, all the adjacent cells use same frequency, and users in the center edge have lower SINR values compared to the other methods. SINR values of the EB_{DSFR} is less than SFR and FFR methods. Cell edge users of the EB_{DSFR} and SFR must transmit maximum power level to achieve maximum throughput rates. This cause Low SINR levels for the proposed scheme.

In figure 6.15, I showed total number of resource blocks (W_i) in the reference cells (Cell 1) of our proposed scheme EB_{DSFR} and other ICI techniques in the literature that are Reuse-1, Reuse-3, SFR and FFR. For these comparisons, I took the $R_C W_B(i)$ constant as 8 for all the simulated techniques. This means that, reference cell is the receiver cell (R_C) that has the highest MPDOR value and other 6 cells can be donor cell according to their $W_L(i)$ values. In every TTI R_C takes 8 RBs from donor cell to allocate its own users. Other techniques are constant RBs and all of them have less RBs compared to my proposed technique. When I look at the FFR technique, RBs values increase when the α values increase. In the FFR method, cell center zone uses frequency reuse-1 method and cell edge zone uses frequency reuse-3 method. And when α increases, number of cell center RBs increases and number of cell edge RBs decreases. For

Reuse3, receiver cell has the smallest number of RBs. Because it can use just 1/3 of the available spectrum. EB_{DSFR} has the highest number of RBs and it has 108 RBs in each TTI. Furthermore, SFR and Reuse-1 methods have 100 RBs in each TTI.

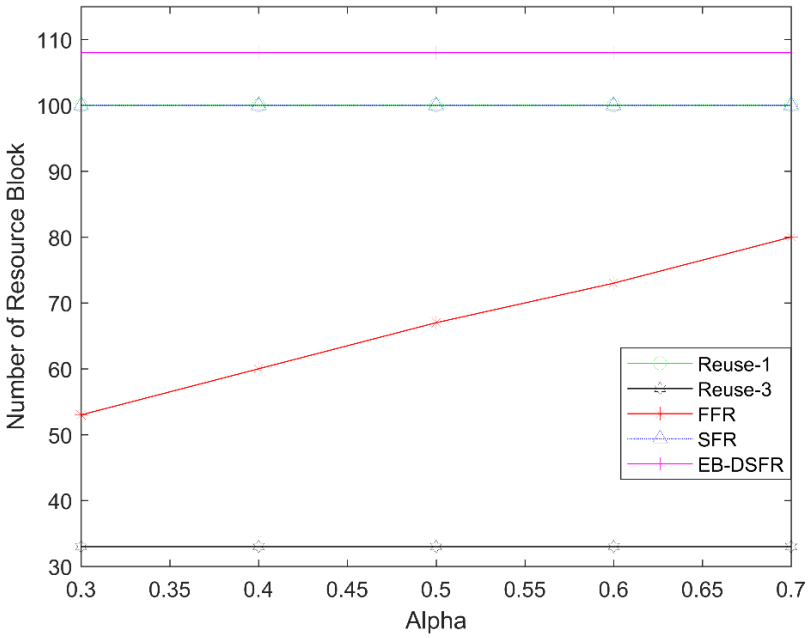

Figure 6.15: Number of resource blocks in the reference cell for Reuse-1, Reuse-3, FFR, SFR and EB_{DSFR} with different α values.

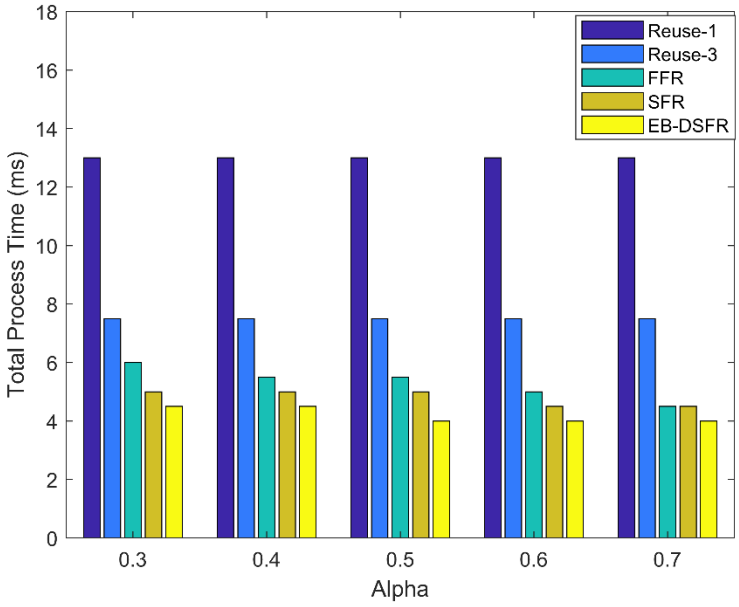

Figure 6.16: Total process time for Reuse-1, Reuse-3, FFR, SFR and EB_{DSFR} with different α values

In figure 6.16, total process time are shown for Reuse-1, Reuse-3, FFR, SFR and EB_{DSFR} with different α values. For determining the total process time, I supposed that every user has service flow with a traffic of 50 Megabyte video stream. When all the users in the cell reach 50 Megabyte total data, I measured the total time. Our proposed scheme has the best performance for allocating the data. The reason of this, EB_{DSFR} has more RBs in one slot time. In addition, Reuse-3 method has worst performance because it has fewer RBs.

6.2 COMPARISON WITH REFERENCE TECHNIQUES

In this scenario I compared our proposed algorithm (EB_{DSFR}) with the reference techniques [11]. The average throughput, cell-edge throughput and cell-center throughput of the reference cell, user's fairness [29], average user delays, average user PDR and dissatisfaction percentages are considered as major referencing elements for performance evaluation. I took account of Dynamic Inter-cellular Bandwidth Fair Sharing FFR and Dynamic Inter-cellular Bandwidth Fair Sharing Reuse-3 as the reference scheme for performance comparison with the proposed technique EB_{DSFR}.

6.2.1 Comparison According to Throughput

In the Table 6.3, numerical values of the comparisons are shown.

Table 6.3: Simulation Results for $EB_{DSFR,}$ FFR_{DIBFS} and $Reuse3_{DIBFS}$ with different α values.

Average User Throughput (Mbps)					
	α=0.3	α=0.4	α=0.5	α=0.6	α=0.7
EB_{DSFR}	6.76	7.02	7.24	7.50	7.68
FFR_{DIBFS}	4.87	5.44	5.97	6.49	7.01
$Reuse3_{DIBFS}$	3.60	3.60	3.60	3.60	3.60
Average Cell Center User Throughput (Mbps)					
	α=0.3	α=0.4	α=0.5	α=0.6	α=0.7
EB_{DSFR}	5.98	7.33	8.85	10.4	11.9
FFR_{DIBFS}	6.23	7.86	9.40	11.0	12.6

$Reuse3_{DIBFS}$	3.69	3.69	3.69	3.69	3.69
Average Cell Edge User Throughput (Mbps)					
	α=0.3	α=0.4	α=0.5	α=0.6	α=0.7
EB_{DSFR}	7.63	6.71	5.63	4.59	3.48
FFR_{DIBFS}	3.52	3.03	2.54	1.92	1.43
$Reuse3_{DIBFS}$	3.51	3.51	3.51	3.51	3.51
Fairness Percentage (%)					
	α=0.3	α=0.4	α=0.5	α=0.6	α=0.7
EB_{DSFR}	97	98	95	87	77
FFR_{DIBFS}	97	98	96	88	78
$Reuse3_{DIBFS}$	99	99	99	99	99

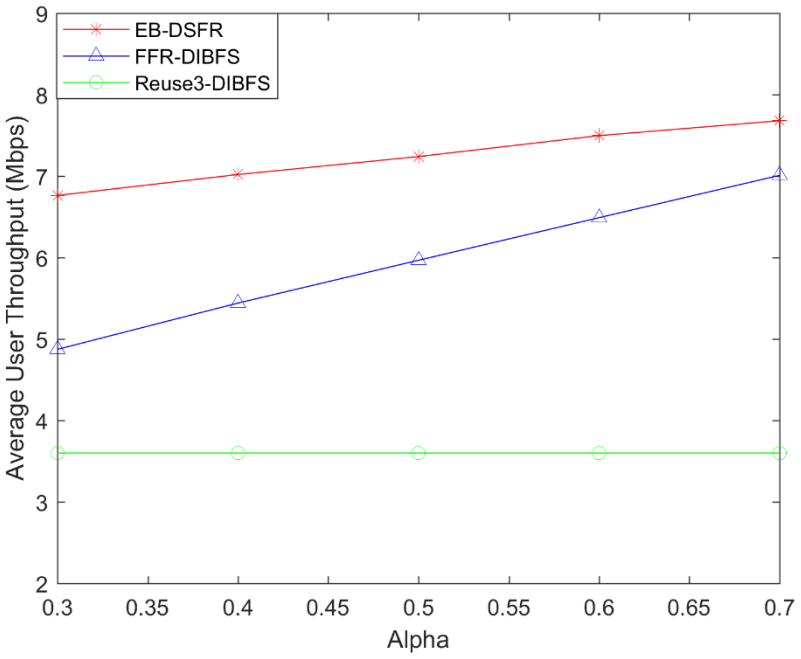

Figure 6.17: Average user throughput for $EB_{DSFR,}$ FFR_{DIBFS} and $Reuse3_{DIBFS}$ with different α values.

First, in figure 6.17, we can see the average user throughput values of our proposed EB_{DSFR} and reference reuse schemes called FFR_{DIBFS} and $Reuse3_{DIBFS}$. Again, I used Round Robin (RR) scheduling algorithm for the reference schemes. Also, for these comparisons, I take the $R_C W_B(i)$

constant as 8 for all the simulated techniques. I just focused on the reference cell (cell 1) and I supposed that, reference cell has the highest MPDOR (receiver cell) and other 6 cells can be donor cell according to their $W_L(i)$ values. For $Reuse3_{DIBFS}$, users have a less average throughput because of the less RBs. It can use just 1/3 of the available spectrum. When we look at the FFR_{DIBFS} technique, average throughput values increase when the α values increase. When I compare FFR_{DIBFS} with the $Reuse3_{DIBFS}$, users have more average throughput values and it changes between 10% and 30%. We can see from the figure, EB_{DSFR} techniques are most efficient techniques in terms of the user average throughput. Because in the EB_{DSFR} method, all the available spectrum can be used. In addition to this, less inter-cell interference increases SINR for the users and user average throughput increases.

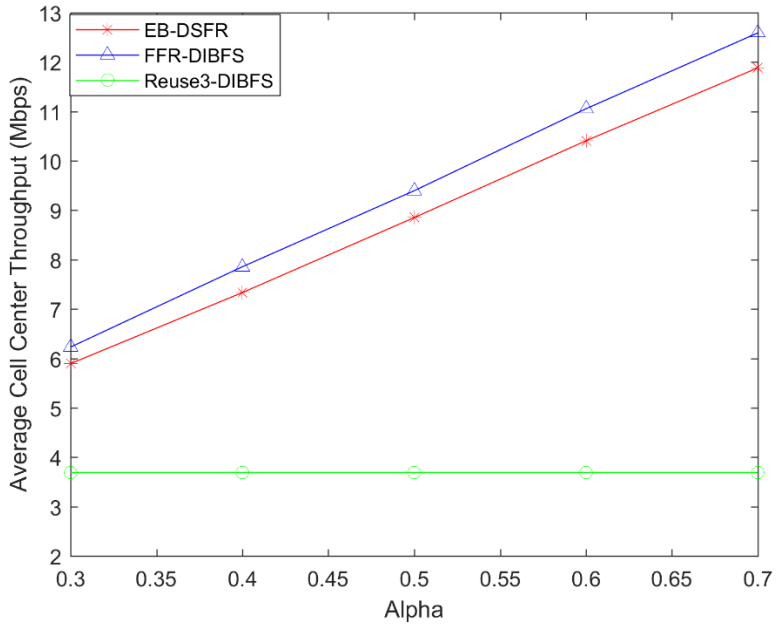

Figure 6.18: Average cell center user throughput for EB_{DSFR}, FFR_{DIBFS} and $Reuse3_{DIBFS}$ with different α values.

As we see in figure 6.18, for EB_{DSFR} and FFR_{DIBFS} when α increases average cell center user throughput increases because number of cell center RBs increases. This means that, more resources can be allocated to user and they can access more RBs in one slot time. The difference is that, FFR_{DIBFS} has better performance than EB_{DSFR} and $Reuse3_{DIBFS}$. Because in the EB_{DSFR} method, cell center user shares same bandwidth with cell edge of the neighboring cells. However, in FFR_{DIBFS} method, cell center user does not share same bandwidth with cell edge of the neighboring cells. They share same bandwidth with cell center of the neighboring cells. The distance between them is more and they have better SINR values. So, average cell center

user throughput is better for the FFR_{DIBFS}. As I mentioned before $Reuse3_{DIBFS}$ average cell center user throughput is constant, and it has worst performance.

In figure 6.19, we can obviously see that. when α increases average cell edge user throughput decreases for FFR_{DIBFS} and EB_{DSFR}. The reason is that, number of cell edge RBs decreases when α increases. The cell edge users FFR_{DIBFS} has bad performance because of the available bandwidth. EB_{DSFR} provides twice throughput rates than the FFR_{DIBFS}. $Reuse3_{DIBFS}$ method has best performance when α is 0.7 values.

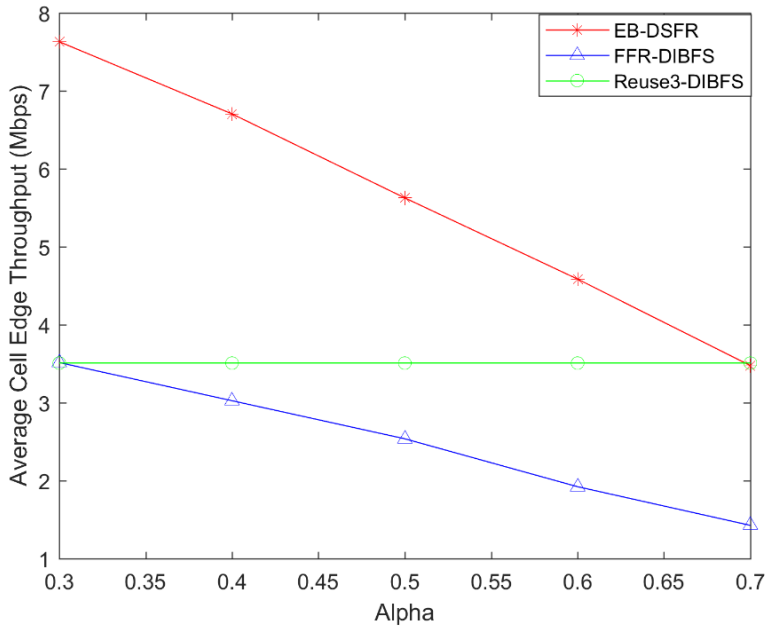

Figure 6.19: Average cell edge user throughput for EB_{DSFR}, FFR_{DIBFS} and $Reuse3_{DIBF}$S with different α values.

As we see in figure 6.20, $Reuse3_{DIBFS}$ technique has the highest throughput fairness index among the frequency reuse techniques. In $Reuse3_{DIBFS}$, because of inter-cell interference is removed, all the users have almost the same throughput rates, and this increases the fairness index. For EB_{DSFR} when α is 0.4, cell edge has more RBs than the cell center but, cell center users have better SINR. So, average cell center and cell edge user's throughput are balanced for this reason. With the increase of the α value, RBs are increase for the cell center, and fairness index decreases for EB_{DSFR} and FFR_{DIBFS} techniques. In the simulation I use Round Robin (RR) scheduling algorithm for the reference techniques and we can see that RR is fairer than our proposed technique that used EBPS as a scheduler algorithm. As we see in figure 6.20, FFR_{DIBFS} is fairer than my proposed algorithm EB_{DSFR}. For FFR_{DIBFS}, I used RR scheduler technique and

we know that in the RR method RBs are assigned to each user in equal portion and in circular order without priority.

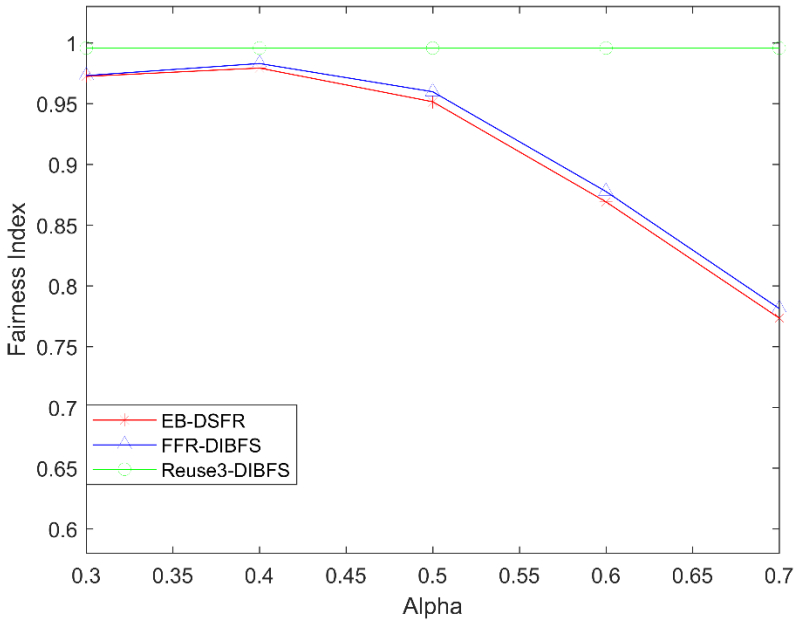

Figure 6.20: Fairness index for EB_{DSFR}, FFR_{DIBFS} and $Reuse3_{DIBFS}$ with different α values.

6.2.2 Comparison According to Delay

In figure 6.21, we can see that, mean users delay for EB_{DSFR}, FFR_{DIBFS} and $Reuse3_{DIBFS}$ for different α values.

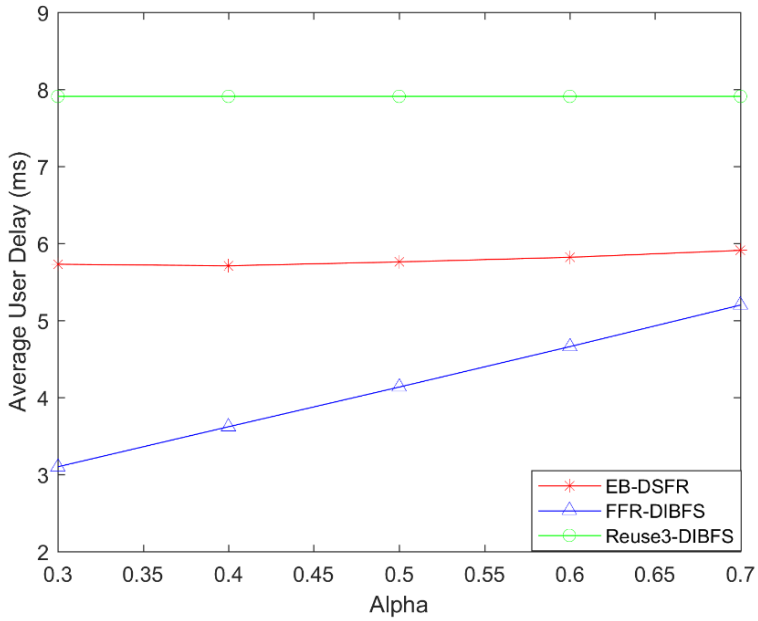

Figure 6.21: Average user delay for EB_{DSFR}, FFR_{DIBFS} and $Reuse3_{DIBFS}$ with different α values

In each technique, there are 10 users in the simulation medium and 5 of them are in the cell center and 5 of them are in the cell edge. When the α increases the delay of FFR_{DIBFS} increases directly proportional because of the increasing number of RBs in the queue. Also, EB_{DSFR} and $Reuse3_{DIBFS}$ have constant RBs that are in the queue. For this reason, delays are almost constant. Although, EB_{DSFR} has more delay than the FFR_{DIBFS}, it provides better throughput values.

In figure 6.22, we can see that, mean cell center users delay for EB_{DSFR}, FFR_{DIBFS} and $Reuse3_{DIBFS}$ for different α values. When the α increases the delay of EB_{DSFR} and FFR_{DIBFS} increase. The reason of this situation, when α values increases, the number of RBs increase in the cell center. For $Reuse3_{DIBFS}$, RBs are constant again. The delays of EB_{DSFR} and FFR_{DIBFS} techniques are approximately same for all α values as seen in the figure. After α=0.55 EB_{DSFR} and FFR_{DIBFS} have more delays than the $Reuse3_{DIBFS}$ technique.

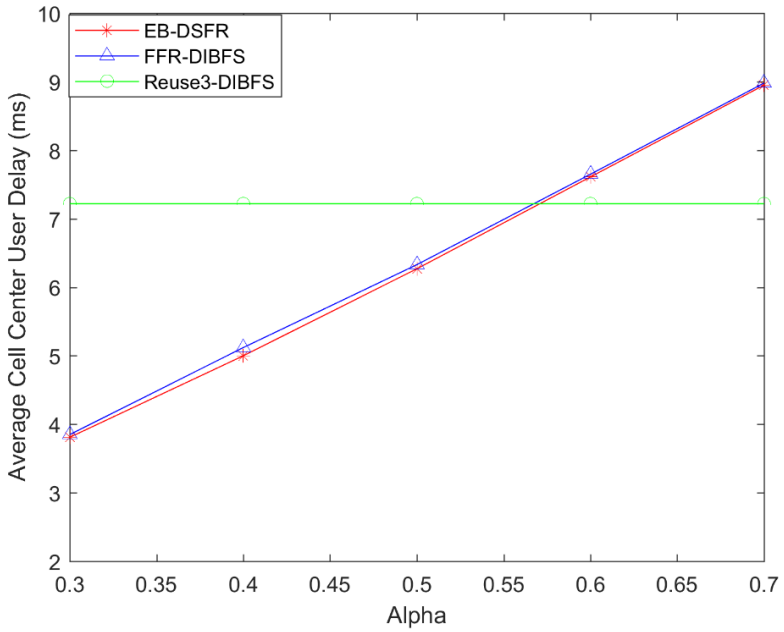

Figure 6.22: Average cell center user delay for EB_{DSFR}, FFR_{DIBFS} and $Reuse3_{DIBFS}$ with different α values.

As we see in figure 6.23, when the α increases the delay of EB_{DSFR} and FFR_{DIBFS} decrease because of the decreasing number of RBs. FFR_{DIBFS} techniques are less delays from the EB_{DSFR}. It uses 1/3 of the RBs in the cell edge and there are less RBs in the queue. This means that, less process time needed to execute. In addition to this, $Reuse3_{DIBFS}$, RBs are constant again and delay are also constants.

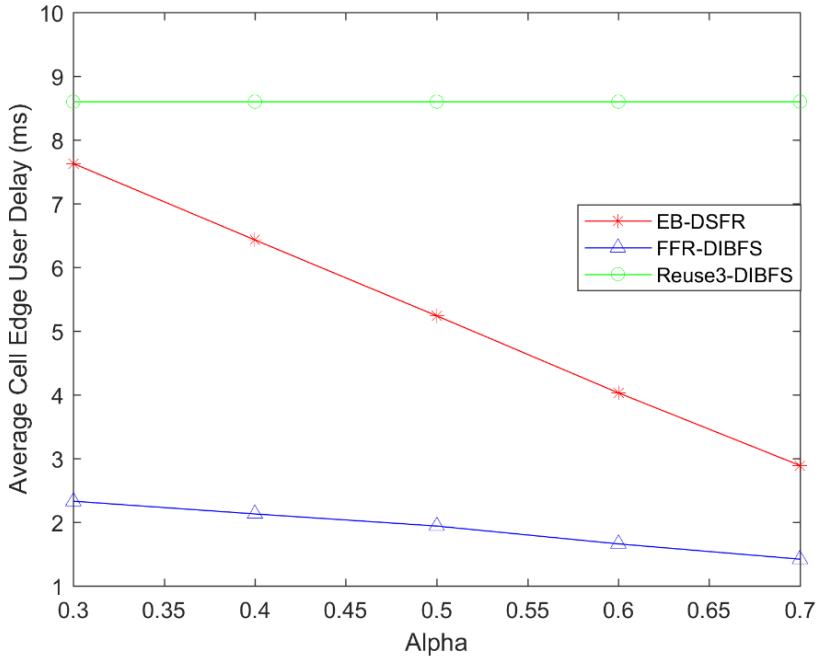

Figure 6.23: Average cell edge user delay for EB_{DSFR}, FFR_{DIBFS} and $Reuse3_{DIBFS}$ with different α values.

6.2.3 Comparison According to PDOR Percentage

In figure 6.24, we can see that, mean user PDR percentages for EB_{DSFR}, FFR_{DIBFS} and $Reuse3_{DIBFS}$ for different α values.

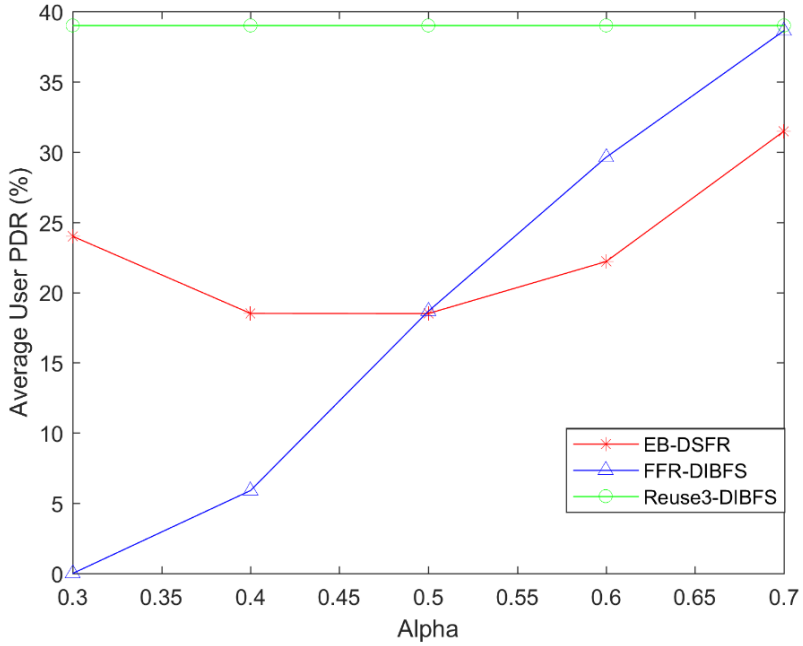

Figure 6.24: Average user PDR (%) for EB_{DSFR}, FFR_{DIBFS} and $Reuse3_{DIBFS}$ with different α values.

When the α increases the PDR (%) of FFR_{DIBFS} increases directly proportional because of the increasing number of RBs in the queue. It changes from 0% to 38.63%. Also, EB_{DSFR} has more PDR % up to α=0.5 compared to the FFR_{DIBFS}. After this value PDR % of the EB_{DSFR} becomes smaller than the FFR_{DIBFS}. This is caused by the number of total RBs of the EB_{DSFR} is more than the number of total RBs of the FFR_{DIBFS}. So, average PDR values of EB_{DSFR} can be higher than the FFR_{DIBFS}. In addition, $Reuse3_{DIBFS}$ have constant RBs that are in the queue. For this reason, PDR percentages are almost constant. Although, EB_{DSFR} has more PDR % for some cases than the FFR_{DIBFS}, it provides better throughput values because of the number of RBs.

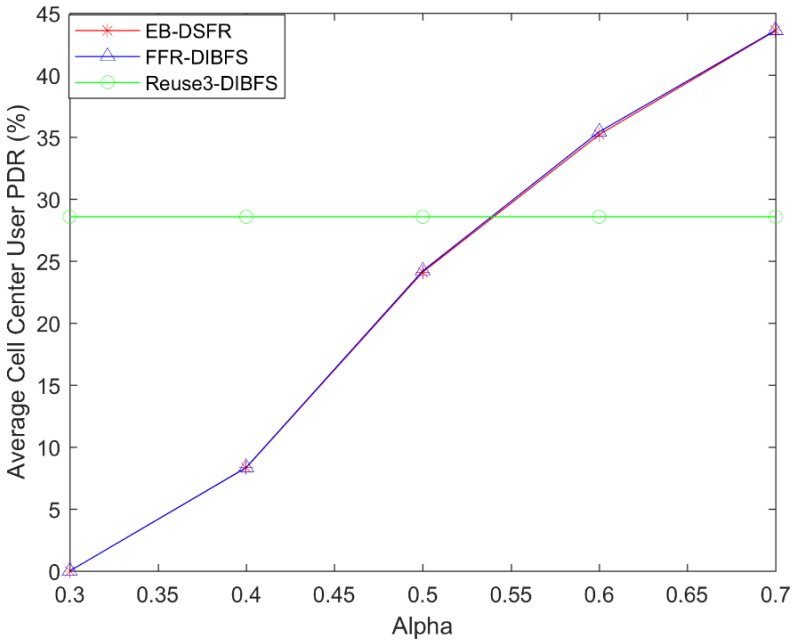

Figure 6.25: Average cell center user PDR (%) for EB_{DSFR}, FFR_{DIBFS} and $Reuse3_{DIBFS}$ with different α values.

As we see in figure 6.25, when the α increases the PDR % of EB_{DSFR} and FFR_{DIBFS} increase. The reason of this, when α values increases, the number of RBs increase in the cell center and delays are also increasing. The PDR percentages of EB_{DSFR} and FFR_{DIBFS} techniques are approximately same for all α values as seen in the figure. Because, they have approximately same delays for all α. For $Reuse3_{DIBFS}$, RBs are constant again and delays and PDR values also constant.

We can see in figure 6.26, when the α increases the PDR % of EB_{DSFR} decreases because of the decreasing number of RBs and delays. At the same time, FFR_{DIBFS} techniques has no RBs in delay outage. It uses 1/3 of the RBs in the cell edge and there are less RBs in the queue. After

α reaches 0.6 value EB_{DSFR} has no delay because of the decreasing number of RBs. Finally, $Reuse3_{DIBFS}$, RBs are constant as 50%.

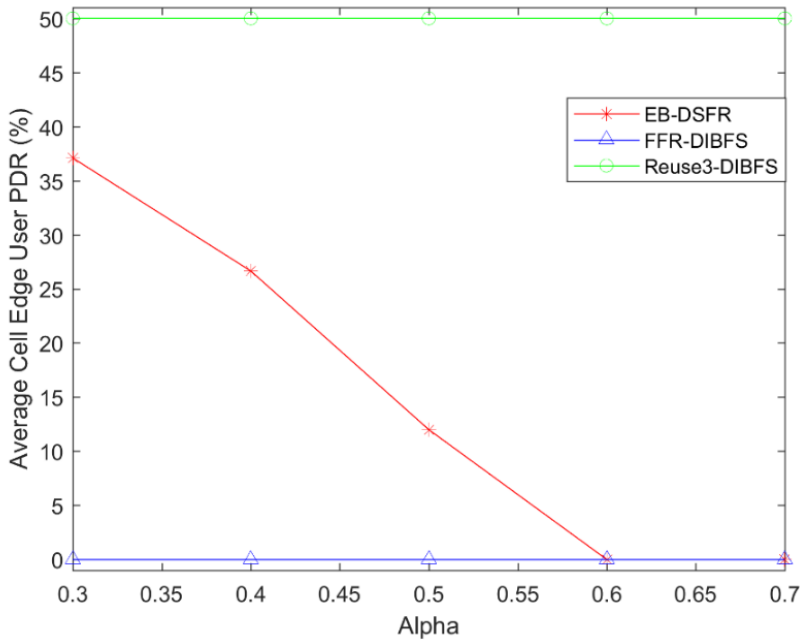

Figure 6.26: Average cell edge user PDR (%) for EB_{DSFR}, FFR_{DIBFS} and $Reuse3_{DIBFS}$ with different α values.

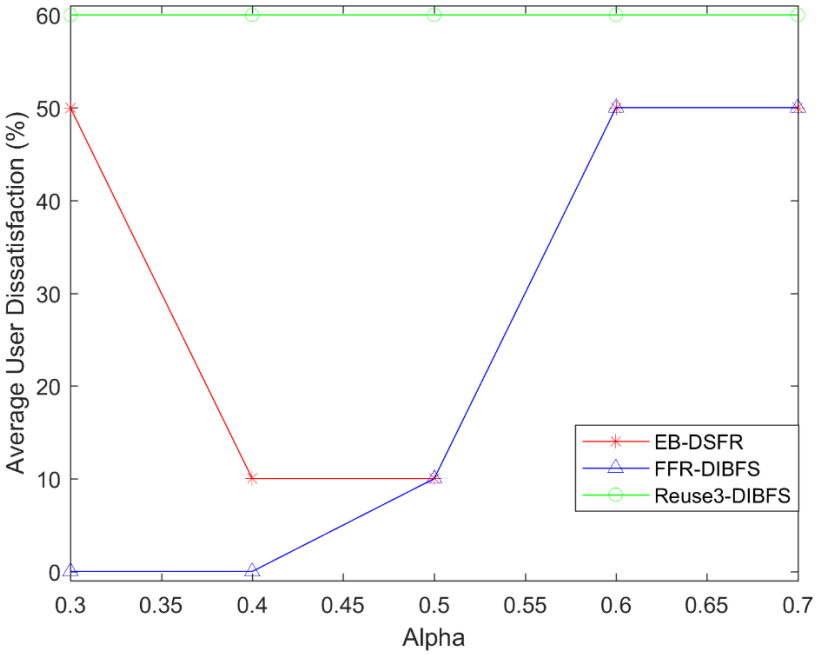

Figure 6.27: Average user dissatisfaction (%) for EB_{DSFR}, FFR_{DIBFS} and $Reuse3_{DIBFS}$ with different α values.

In figure 6.27, we can see that, average user dissatisfaction percentages for EB_{DSFR}, FFR_{DIBFS} and $Reuse3_{DIBFS}$ for different α values. FFR_{DIBFS} has best dissatisfaction ratio up to α=0.5 and after that value, EB_{DSFR} has same dissatisfaction ratio with the FFR_{DIBFS}. $Reuse3_{DIBFS}$ has constant dissatisfaction ratio as a 60%. Users are more satisfied according to FFR_{DIBFS} as a delay performance but, as a throughput performance they are more dissatisfied than the EB_{DSFR} users.

6.2.4 Comparison According to SNIR

In this scenario, I compared our proposed algorithm EB_{DSFR} with the reference techniques that are Dynamic Inter-cellular Bandwidth Fair Sharing FFR (FFR_{DIBFS}) and Dynamic Inter-cellular Bandwidth Fair Sharing Reuse-3 ($Reuse3_{DIBFS}$). I took user's SINR as major referencing elements for performance of the schemes. As like reference techniques have, I focused on performance of a reference cell that is cell 1. Cell 1 is the center cell and other 6 cells surround it.

In figure 6.28, we can see the average user SINR values of our proposed EB_{DSFR} and reference reuse techniques FFR_{DIBFS} and $Reuse3_{DIBFS}$. As I mentioned above; In $Reuse3_{DIBFS}$ method, all the adjacent cells use different frequency, and all the users have very high SINR values. In the FFR_{DIBFS} method, cell center zone uses frequency reuse-1 method and cell edge zone uses frequency reuse-3 method. Also, cell center and cell edge use different frequency band, and this provides better SINR values compared to EB_{DSFR}.

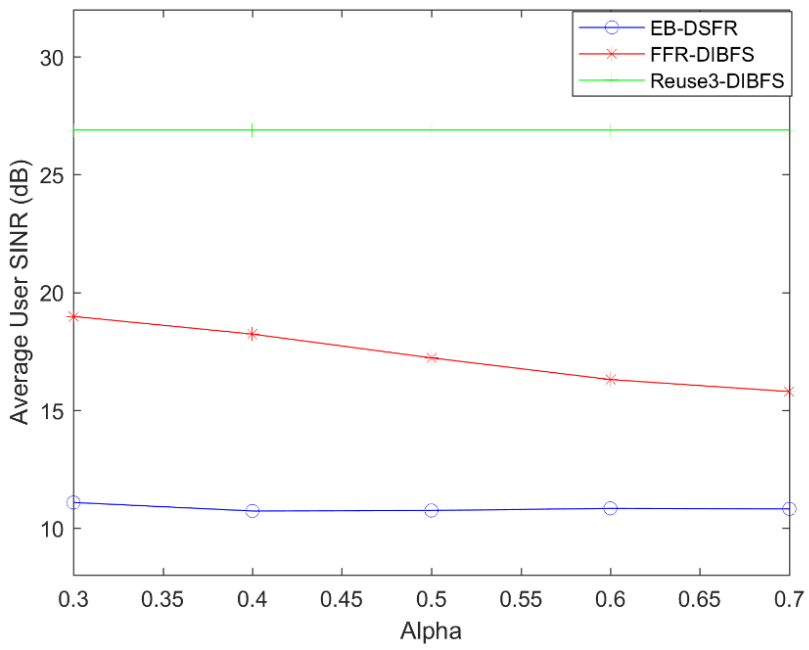

Figure 6.28: Average user SINR for EB_{DSFR}, FFR_{DIBFS} and $Reuse3_{DIBFS}$ with different α values.

When we look at the SINR values of the EB_{DSFR}, in the cell center band, frequency spectrum is allocated lower transmission power because cell center user shares same bandwidth with cell edge of the neighboring cells cell center users have good SINR values but, cell edge users have low SINR values. EB_{DSFR} has less SINR values compared to the reference techniques, but it uses all the available spectrum and has better throughput values.

As we seen in the figure 6.29, $Reuse3_{DIBFS}$ method has the highest cell center SINR values. As I explained before, all neighboring cell use different frequency, and this causes high SINR values but, lower throughput values. Our proposed method EB_{DSFR} has worst SINR values as we see. In the EB_{DSFR} method, cell center users use same bandwidth with the neighboring cells' cell edges, but in FFR_{DIBFS} method it is not like this. They use same bandwidth with neighboring cells' cell center. Because of the more distance, they have better SINR values than the EB_{DSFR} method. In addition to this, when α increases, the SINR values of the EB_{DSFR} and FFR_{DIBFS} decreases. Because, cell center expands and users who locates in the cell center are away from the base station. This causes less average SINR values.

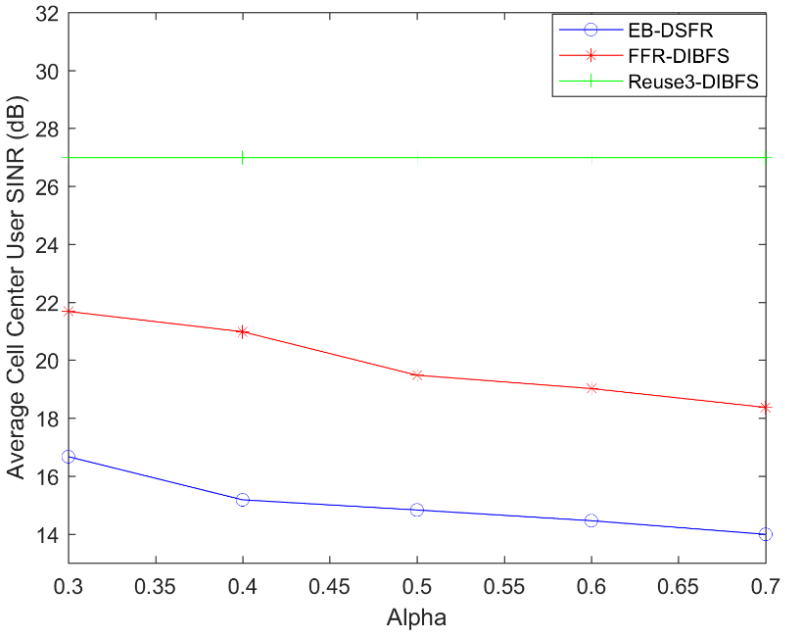

Figure 6.29: Average cell center user SINR for EB_{DSFR}, FFR_{DIBFS} and $Reuse3_{DIBFS}$ with different α values.

In figure 6.30, we can see that, the SINR values of the EB_{DSFR} is less than FFR_{DIBFS} and $Reuse3_{DIBFS}$ methods. Cell edge users of the EB_{DSFR} must transmit maximum power level to achieve maximum throughput rates. This cause Low SINR levels for the proposed scheme.

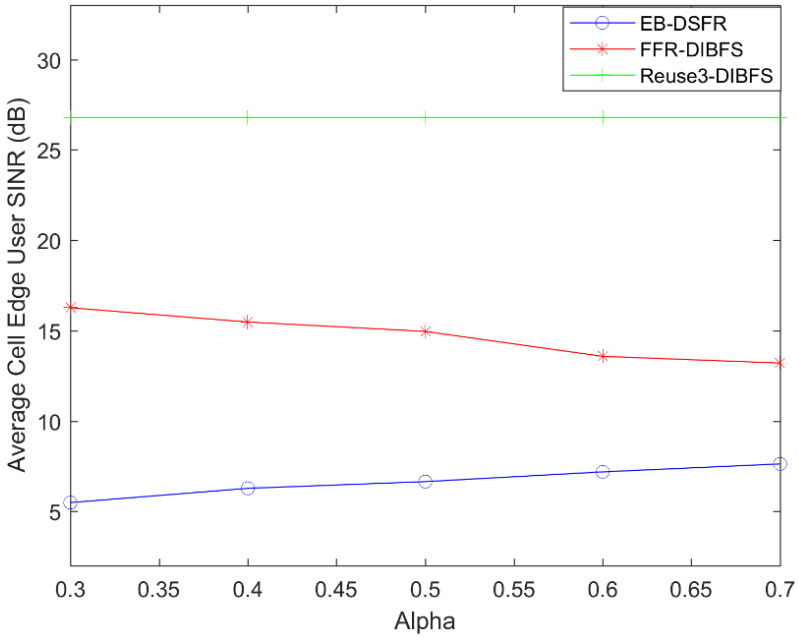

Figure 6.30: Average cell edge user SINR for EB_{DSFR}, FFR_{DIBFS} and $Reuse3_{DIBFS}$ with different α values.

6.2.5 Comparison According to Resource Blocks (RB)

In figure 6.31, I showed total number of resource blocks (W_i) in the reference cells (Cell 1) of our proposed scheme EB_{DSFR} and reference reuse schemes FFR_{DIBFS} and $Reuse3_{DIBFS}$.

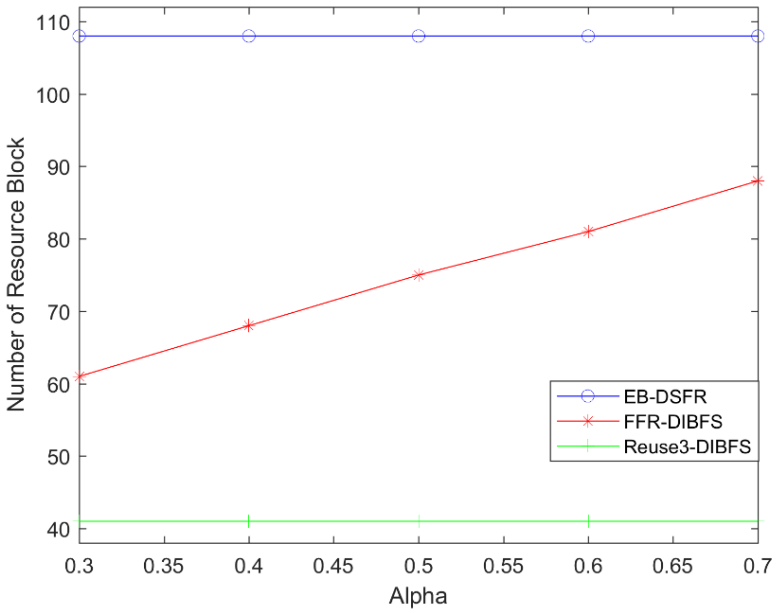

Figure 6.31: Number of resource blocks in the reference cell for EB_{DSFR}, FFR_{DIBFS} and $Reuse3_{DIBFS}$ with different α values.

For these comparisons, I took the $R_C W_B(i)$ constant as 8 for all the simulated techniques. This means that, reference cell is the receiver cell (R_C) that has the highest MPDOR value and other 6 cells can be donor cell according to their $W_L(i)$ values. In every TTI R_C takes 8 RBs from D_C to allocate its own users. For $Reuse3_{DIBFS}$, receiver cell has the smallest number of RBs. Because it can use just 1/3 of the available spectrum. When I look at the FFR_{DIBFS} technique, RBs values increase when the α values increase. In the FFR_{DIBFS} method, cell center zone uses frequency reuse-1 method and cell edge zone uses frequency reuse-3 method. And when α increases, number of cell center RBs increases and number of cell edge RBs decreases. But, it does not happen direct proportionally, amount of increment is higher than the decrement. EB_{DSFR} has the highest number of RBs. Because in the EB_{DSFR} method, all the available spectrum is used and in the reference cell 108 RBs are available to allocate to the users.

Table 6.4 depicts the average number of RBs (W_i) in the 7 different cells for different reuse schemes.

Table 6.4: Average number of RBs (W_i) in the clusters for each cell.

	Cell-1	Cell-2	Cell-3	Cell-4	Cell-5	Cell-6	Cell-7
EB-DSFR	108	100	96.8	98.4	98.4	99.2	99.2
FFR_DIBFS	61	51.4	53	50.6	52.2	50.6	52.2
Reuse3_DIBFS	41	32.2	30.6	33	32.2	29.8	32.2

Figure 6.32 depicts the average number of RBs in the 7 different cells for different reuse schemes. In each cell EB_{DSFR} has maximum number of RBs because of the available spectrum usage. EB_{DSFR} uses whole available spectrum and for this reason it has more RBs than the reference schemes. When I look the $FFR_{DIBFS,}$ it uses partial spectrum at the cell edge so, it has less RBs than our proposed scheme. Finally, $Reuse3_{DIBFS}$ uses 1/3 of al spectrum and it has smallest number of RBs. Furthermore, in each scheme, cell 1 has the maximum number of RBs. Cell 1 is the receiver cell and in each TTI it takes some part of RBs of the other cells according to the load.

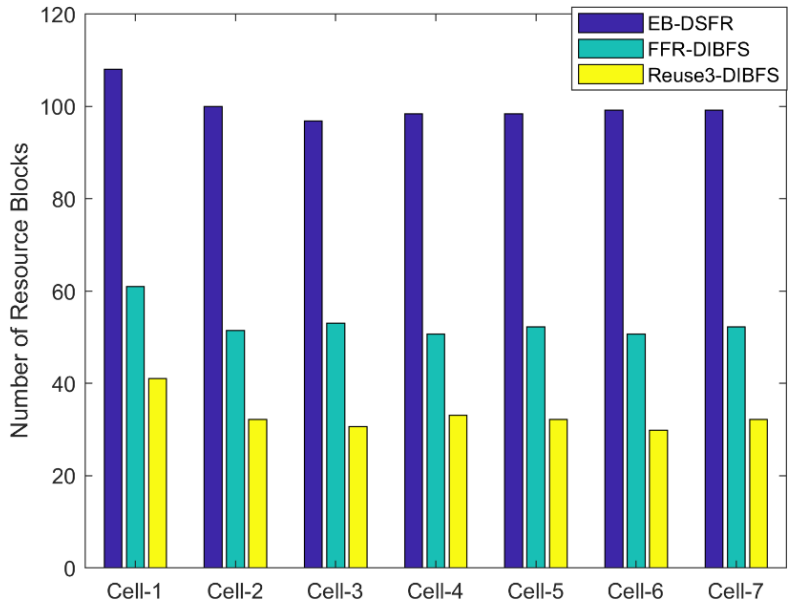

Figure 6.32: Average number of RBs in the 7 different cells for EB_{DSFR}, FFR_{DIBFS} and $Reuse3_{DIBFS}$

Table 6.5 depicts the average number borrowable resource blocks (W_B) in the 7 different cells for different reuse schemes.

Table 6.5: Average number of borrowable resource blocks (W_B) in the clusters for each cell.

	Cell-1	Cell-2	Cell-3	Cell-4	Cell-5	Cell-6	Cell-7
EB-DSFR	8	6.6	6.9	6.9	7.08	7.3	6.62
FFR_DIBFS	8	6.66	7.12	7.1	6.84	7.04	6.66
Reuse3_DIBFS	8	7.6	6.6	7.2	7.1	7.1	7.5

Figure 6.33 respectively shows the average number of borrowable bandwidth W_B in the 7 different cells for different reuse schemes. W_B is the bandwidth or number of resource blocks that R_C can borrow from the D_C. In each TTI, W_B is calculated and the cell which has the highest MPDOR takes the number of RBs as the amount of W_B from the receiver cell (R_C). In this figure we can clearly see that, Cell 1 has the highest RBs because it is the cell that has the highest load.

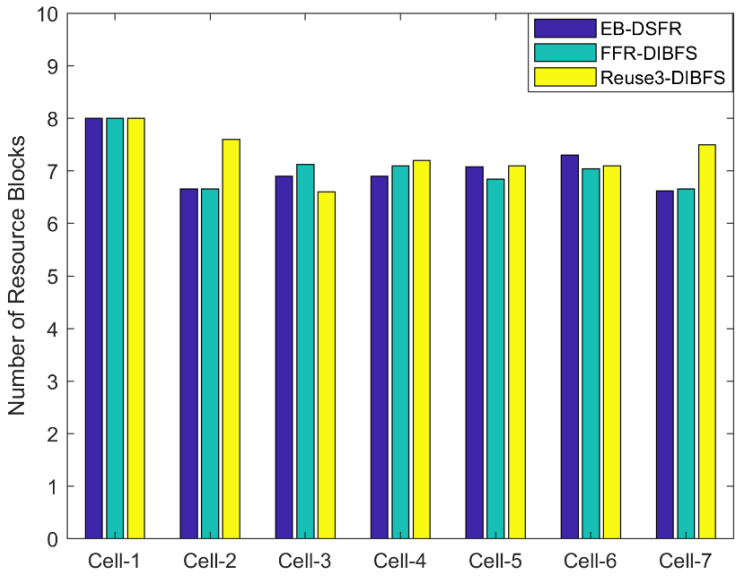

Figure 6.33: Average number of borrowable resource blocks (WB) in each cell for EB_{DSFR}, FFR_{DIBFS} and $Reuse3_{DIBFS.}$

Table 6.6 depicts the average number lendable resource blocks (W_L) in the 7 different cells for different reuse schemes.

Table 6.6: Average number of lendable resource blocks (W_L) in the clusters for each cell.

	Cell-1	Cell-2	Cell-3	Cell-4	Cell-5	Cell-6	Cell-7
EB-DSFR	5.28	11.66	11.46	10.04	10.3	10.54	11
FFR_DIBFS	5.62	10.18	11.16	11.08	10.56	11.84	10.02
Reuse3_DIBFS	6.1	88.	11.4	10.4	9.3	10.6	11

In figure 6.34, we can see the average number of lendable bandwidth W_L in the 7 different cells for different reuse schemes. W_L is the bandwidth or number of resource blocks that R_C can take from the D_C. In each TTI, W_L is calculated and the cell which has the highest W_L gives the number of RBs as the amount of W_L to the receiver cell (R_C). In this figure, we can clearly see that, Cell 1 has the smallest RBs because it is the cell that has the highest load.

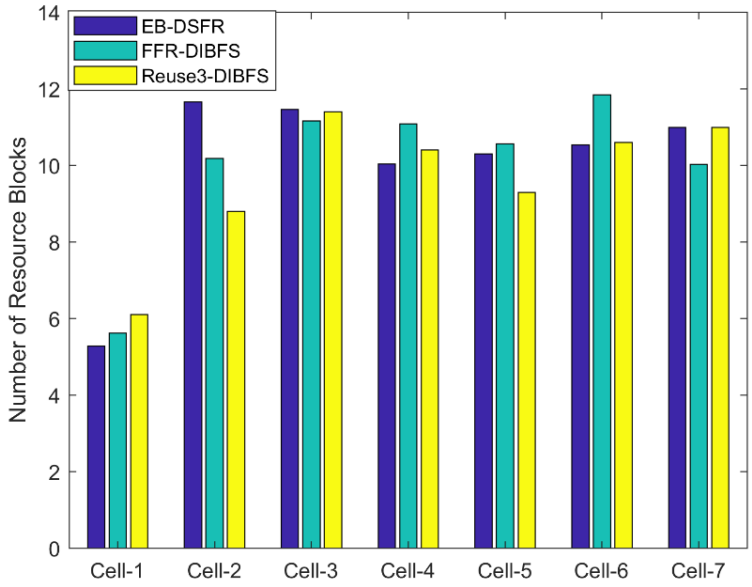

Figure 6.34: Average number of lendable resource blocks (WL) in each cell for EB_{DSFR}, FFR_{DIBFS} and $Reuse3_{DIBFS.}$

In figure 6.35, total process time are shown for EB_{DSFR}, FFR_{DIBFS} and $Reuse3_{DIBFS}$ with different α values. Our proposed scheme has the best performance for allocating the data. For each α values EB_{DSFR} has better performance up to 37.5% than the reference schemes. The reason of this, EB_{DSFR} has more RBs in one slot time and it can reach to total download more quickly than the other methods.

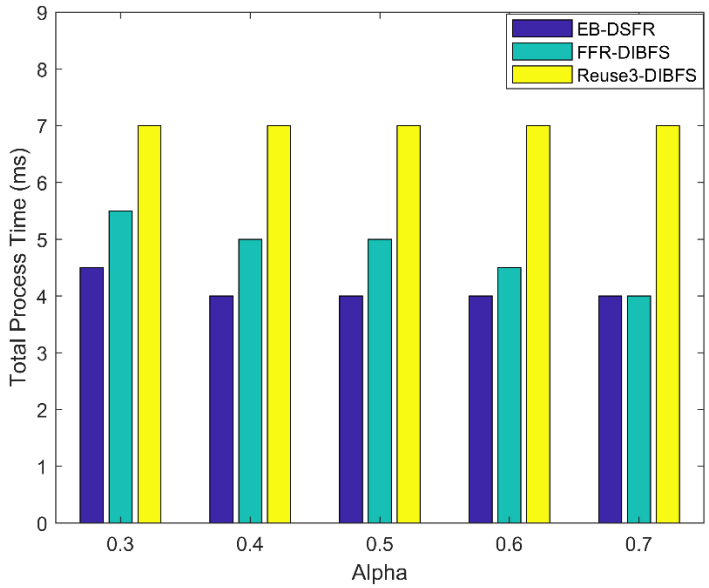

Figure 6.35: Total process time for EB_{DSFR}, FFR_{DIBFS} and $Reuse3_{DIBFS}$ with different α values

7. CONCLUSION

In this thesis, I proposed ICIC technique that maximize the overall system throughput. The proposed technique provides resource sharing between cells, it prevents wasting of the unused resources. In addition to this, by considering user's previous experiments, I gave the priority to users who have poor previous experiments. I also considered SINR and power levels for the users to optimize the proposed algorithm. Furthermore, our proposed algorithm can adjust resources sharing between cells dynamically. I compared our proposed algorithm with frequency reuse methods that are already utilized in the LTE systems and reference methods. I simulated all the methods including our proposed one by using MATLAB and I compared as a numerical analysis. I saw that, our proposed method provides higher average throughput rates than the reference methods between 10% and 30%. Moreover, EB_{DSFR} provides approximately same fairness except Reuse-3 scheme. When I compared the SINR values, our proposed scheme has worse than the reference schemes. But, EB_{DSFR} uses all available spectrum and this disadvantage is eliminated for the throughput levels. When I see the delays, it has more burst delays compared with the FFR_{DIBFS}. As opposite to this, when I restricted the total data that allocated to each user, our proposed scheme has best performance. In the future, I can increase throughput and I can provide better fairness. Also, I can increase SINR by setting the power levels and I will try to minimize average delays.

REFERENCES

[1] Srikanth, P. Murugesa Pandian, and X. Fernando, "Orthogonal frequency division multiple access in WiMAX and LTE: a comparison", *Communications Magazine, IEEE*, vol. SO, no. 9, pp. IS3-161, 2012.

[2] K. Bakanoglu, W. Mingquan, L. Hang, M. Saurabh, "*Adaptive resource allocation in multicast OFDMA systems*," in: Proceedings of Wireless Communications and Networking Conference, IEEE, 2010, pp. 1–6.

[3] G. Giambene, T. A. Yahiya, V. A. Le, K. Grochla, K. Połys, "*Resource management and cell planning in LTE systems*," in Wireless Networking for Moving Objects. Springer, 2014, pp. 177–197.

[4] M. Necker, "*Interference coordination in cellular OFDMA networks*," IEEE Network, vol. 22, pp. 12-19, 2008.

[5] Y. Yu, E. Dutkiewicz, X. Huang, M. Mueck, and G. Fang, "*Performance analysis of soft frequency reuse for inter-cell interference coordination in LTE networks*" IEEE International Symposium on Communications and Information Technologies, pp. 504-509, 2010

[6] G. Boudreau, J. Panicker, N. Guo, R. Chang, N. Wang, and S. Vrzic, "*Interference coordination and cancellation for 4G networks*," IEEE Communications Magazine, vol. 47, pp. 74-81, 2009.

[7] M. Assaad, *"Optimal Fractional Frequency Reuse (FFR) in multicellular OFDMA system*", Vehicular Technology Conference, VTC 2008-Fall. IEEE 68th, 2008.

[8] M. A. AboulHassan, M. Yassin, S. Lahoud, M. Ibrahim, D. Mezher, B. Cousin, E. A. Sourour, "*Classification and Comparative Analysis of Inter-Cell Interference Coordination Techniques in LTE Networks*", 7th International Conference on New Technologies, Mobility and Security (NTMS), Paris, 2015.

[9] 3GPP and Huawei, "*Soft frequency reuse scheme for UTRAN LTE*," in R1-050507, TSG RAN WG1 Meeting#41, Athens, Greece, 2005.

[10] 3GPP and Huawei, "*Further Analysis of soft frequency reuse scheme*," in R1-050841, TSG RAN WG1#42, San Seoul, Korea, 2005.

[11] M. Ezzaouia, C. Gueguen, M. Ammar, S. Baey, X. Lagrange, A. Bouallegue, "*Dynamic Inter- Cell Interference Coordination Techniques for Future Wireless Networks*", 13th IEEE International Conference on Wireless and Mobile Computing, Networking and Communications, Oct 2017, Rome, Italy.

[12] S. Jayasankar, "*Evaluation of Static Frequency Reuse Techniques in OFDM Cellular Networks Using SINR*", International Journal of Scientific & Engineering Research, Volume 6, Issue 2, February-2015, ISSN 2229-5518.

[13] M. Yagcioglu, O. Bayat, "*Experience-Based Packet Scheduler*", ICEMIS '15 Proceedings of the The International Conference on Engineering & MIS, Istanbul, Turkey, September, 2015. ISBN: 978-1-4503-3418-1

[14] G. Giambene, V. A. Le, T. Bourgeau and H. Chaouchi, "*Soft frequency Reuse Schemes for Heterogeneous LTE Systems*," 2015 IEEE International Conference on Communications (ICC), London, 2015, pp. 3161-3166.

[15] Iskandar and H. Nuraini, "*Inter-Cell Interference Coordination with Soft Frequency Reuse Method for LTE Network*," in Proceeding of the 2th International Conference on Wireless and Telematics (ICWT 2016), vol 1, Jogjakarta, Indonesia, 2016.

[16] M. Yassin, "*Inter-cell interference coordination in wireless networks*," Ph.D. dissertation, Université de Rennes 1, 2015.

[17] H. Lei, L. Zhang, X. Zhang, and D. Yang, "*A novel multi-cell ofdma system structure using fractional frequency reuse*," IEEE 18th International Symposium on Personal, Indoor and Mobile Radio Communications. IEEE, 2007, pp. 1–5.

[18] R. K. Jain, D. W. Chiu, and W. R. Hawe, "*A Quantitative Measure of Fairness and Discrimination for Resource Allocation and Shared Computer System,*" Digital Equipment Corporation, Tech. Rep., 1984.

[19] S. Rathi, N. Malik, N. Chahal, S. Malik, "*Throughput for TDD and FDD 4 G LTE Systems*," International Journal of Innovative Technology and Exploring Engineering (IJITEE), ISSN: 2278-3075, Volume-3, Issue-12, May 2014

[20] G. González, M. García-Lozano, S. Ruiz, J. Olmos et al., "*On the need for dynamic downlink intercell interference coordination for realistic long-term evolution deployments*," Wireless Communications and Mobile Computing, vol. 14, no. 4, pp. 409–434, 2014.

[21] E.Dallman, S.Parkvell, and J.Skold,"*4G LTE/LTE Advanced for mobile broadband*", Elseiver, 2011.

[22] N.Himayat, S.Talawar, A.Rao, and R.Soni,"*Interference Management for 4G Cellular Standards[WIMAX\LTE update]*",IEEE Communications Magazine, Vol. 48, no 8,pp.86-92,August 2010.

[23] X. Yang, "*Soft frequency reuse scheme for utran lte,*"," Huawei, 3GPP R1-050507, TSG-RAN1, vol. 41, 2005.

[24] C. Jiming, W. Peng, and Z. Jie, "*Adaptive soft frequency reuse scheme for in-building dense femtocell networks*," China Communications, vol. 10, no. 1, pp. 44–55, 2013.

[25] L. Shu, X. Wen, Z. Liu, W. Zheng, and Y. Sun, "*Queue anlysis of soft frequency reuse scheme in lte-advanced*," in Computer Modeling and Simulation, 2010. ICCMS'10. Second International Conference on, vol. 1. IEEE, 2010, pp. 248–252.

[26] M. Qian, W. Hardjawana, Y. Li, B. Vucetic, X. Yang, J. Shi, "*Adaptive soft frequency reuse scheme for wireless cellular networks*," Vech. Tech., IEEE Transaction on, vol. 64, no. 1, pp. 118–131,

[27] D. Lopez-Perez, I. Guvenc, G. De la Roche, M. Kountouris, T. Q. Quek, and J. Zhang, "*Enhanced intercell interference coordination challenges in heterogeneous networks*," IEEE Wireless Communications, vol. 18, no. 3, 2011.

[28] J. Wang, X. She and L. Chen, "*Enhanced dynamic inter-cell interference coordination schemes for LTE-advanced*," In Vehicular Technology Conference (VTC Spring), pp. 1-6, 2012.

[29] J. Wang, J. Liu, D.Wang, J. Pang and G. Shen, "*Optimized fairness cell selection for 3GPP LTE-A macro-pico HetNets*," In Vehicular Technology Conference (VTC Fall), pp. 1-5, 2011.

[30] J. Wang, J. Weitzen, V. Sevindik, O. Bayat, M. Li, "*Joint interference coordination approach in femtocell networks for QoS performance optimization*", International Journal of Communication Systems, 2017

[31] E. Tuomaala, H. Wang, "*Effective SINR approach of link to system mapping in ofdm/multicarrier mobile network*", IEEE International Conference on 2nd Asia Pacific Conference on Mobile Technology, Applications and Systems, Guangzhou, China, 2005.

[32] R. Y. Chang, Z. Tao, J. Zhang, and C.-C. J. Kuo, "*A graph approach to dynamic fractional frequency reuse (FFR) in multi-cell OFDMA networks*," in Proc. of the IEEE International Conference on Communications, Dresden, Germany, 2009.

[33] K. Doppler, C. Wijting, and K. Valkealahti, "*Interference aware scheduling for soft frequency reuse*," in Proc. IEEE VTC Spring, Apr. 2009, pp. 1–5.

[34] M. Yagcioglu, O. İleri, S. Ergut, O. Bayat, "*Experience-Based Packet Scheduler*", U.S Patent WO2014129994, Aug. 29, 2014.

[35] J. Wang, J. Weitzen, V. Sevindik, O. Bayat, M. Li, "*Dynamic Centralized Interference Coordination in Femto Cell Network with QoS Provision*", Latest Trends on Communications, Proceedings of the 18th International Conference on Communications (Part of CSCC'14). 2014.

[36] Penttinen, J. "*The LTE/SAE Deployment Handbook"*, John Wiley & Sons, Ltd, Chichester, 2011

[37] Holma, H. and Toskala, A. "*LTE for UMTS: Evolution to LTE-Advanced"*, Ch. 10, John Wiley & Sons, Ltd, Chichester, 2011

[38] C. Cox, "Orthogonal Frequency Division Multiple Access" *An Introduction to LTE, LTE, LTE Advanced , Sae and 4G Mobile Communications* 1st UK: Wiley, 2012, pp 61-72

[39] M. Hina and S. Sohaib, "*Centralized dynamic frequency allocation for cell-edge demand satisfaction in fractional frequency reuse networks*," Telecommunication Systems, pp. 1–14, 2017.

[40] D. L´opez-P´erez, X. Chu, A. V. Vasilakos, H. Claussen, "*Power minimization based resource allocation for interference mitigation in OFDMA femtocell networks*," *Selected Areas in Communications, IEEE Journal on*, vol. 32, no. 2, pp. 333–344, 2014.

[41] Kshatriya, S.N.S. Kaimalettu, S. Yerrapareddy, S.R. Milleth and Nadeem Akhtar, "*On interference management based on subframe blanking in heterogeneous LTE networks*," In Communication Systems and Networks (COMSNETS), pp. 1-7, 2013.

[42] S. Moon, B. Kim, S. Malik, C. You, H. Liu, J.H. Kim, J. Kim, and I. Hwang, "*Cell Selection and Resource Allocation for Interference Management in a Macro-Picocell Heterogeneous Network*," Wireless Personal Communications ,vol. 83, no. 3, pp. 1887-1901, 2015

[43] Xu, Z., Li, G.Y., Yang, C., Zhu, X.: "*Throughput and optimal threshold for FFR schemes in OFDMA cellular networks*", IEEE Trans. Wirel. Commun., 2012, 11, (8), pp. 2776–2785

[44] C. Guéguen and S. Baey, "*Comparison study of resource allocation strategies for ofdm multimedia networks*," Journal of Electrical and Computer Engineering, vol. 2012, p. 3, 2012.

[45] X. Zhang, C. He, L. Jiang, and J. Xu, "*Inter-cell interference coordination based on softer frequency reuse in OFDMA cellular systems*," in Proc. 2008 IEEE Int. Conf. Neural Networks and Signal Processing, pp. 270– 275

[46] W. Wang, L. Xu, Y. Zhang, and J. Zhong, "*A novel cell-level resource allocation scheme for OFDMA system,*" in Proc. 2009 Commun. and Mobile Computing, pp. 287–292.

[47] L. Chen and D. Yuan, "*Generalized frequency reuse schemes for OFDMA networks: Optimization and comparison*," in Proc. IEEE 71st Veh. Technol. Conf. (VTC Spring), May 2010, pp. 1–5.

[48] D. González G, M. Garcia-Lozano, S. R. Boque, and D. S. Lee, "*Optimization of soft frequency reuse for irregular LTE macrocellular networks,*" IEEE Trans. Wireless Commun., vol. 12, no. 5, pp. 2410–2423, May 2013.

[49] F. Jin, R. Zhang, and L. Hanzo, "*Fractional frequency reuse aided twin-layer femtocell networks: Analysis, design and optimization*," IEEE Trans. Commun., vol. 61, no. 5, pp. 2074–2085, May 2013.

[50] B. M. Hambebo, M. M. Carvalho, and F. M. Ham, "*Performance evaluation of static frequency reuse techniques for OFDMA cellular networks*," in Proc. IEEE 11th Int. Conf. Netw., Sens. Control, 2014, pp. 355–360.

[51] S. Kumar, S. Kalyani, and K. Giridhar, "*Optimal design parameters for coverage probability in fractional frequency reuse and soft frequency reuse*," IET Commun., vol. 9, no. 10, pp. 1324–1331, 2015

[52] X. Yang, "*A multilevel soft frequency reuse technique for wireless communication systems*," IEEE Communications Letters, vol. 18, no. 11, pp. 1983–1986, 2014.

[53] Z. Xie and B. Walke, "*Frequency reuse techniques for attaining both coverage and high spectral efficiency in ofdma cellular systems*," in IEEE Wireless Communications and Networking Conference (WCNC), 2010.

[54] Y. Yu, E. Dutkiewicz, X. Huang, and M. Mueck, "*Adaptive power allocation for soft frequency reuse in multi-cell lte networks*," in International Symposium on Communications and Information Technologies (ISCIT), 2012, pp. 991–996

[55] G. Lv, S. Zhu, and H. Hui, "*A distributed power allocation algorithm with inter-cell interference coordination for multi-cell ofdma systems*," in IEEE Global Telecommunications Conference (GLOBECOM), 2009.